A Molecular Characterization of Agonists That Bind to Hco-UNC-49, a GABA-gated Chloride Channel From *Haemonchus contortus*

By

Mark D. Kaji

A Thesis Submitted in Partial Fulfillment

Of the Requirements for the Degree of

Masters of Science

In

The Faculty of Science

Applied Bioscience

University of Ontario Institute of Technology

November, 2012

Certification of Approval

Copyright Agreement

Abstract

Haemonchus contortus is a blood feeding parasitic nematode infecting ruminants causing anemia and poor health at great economic cost. The ability to pharmaceutically control infection has been challenged by the rapid development and spread of drug resistance. The discovery of new targets is therefore required for sustainable parasite control. UNC-49 is a nematode ligand-gated ion channel that plays an important role in muscle contraction required for normal locomotion. However, little is known regarding its sensitivity to different agonists and how they interact with the binding site. This thesis describes an investigation into the efficacy of a range of classical GABA receptor agonists on Hco-UNC-49 expressed in *Xenopus* oocytes. The results of our electrophysiological recordings indicate that there is a size requirement for full agonism of the Hco-UNC-49 binding site. Furthermore, a number of molecules that are known to act on vertebrate GABA receptors have no effect on Hco-UNC-49. This suggests that the binding site of nematode GABA receptors does exhibit some unique properties. These findings could possibly be exploited to develop new drugs that specifically target GABA receptors from parasitic nematodes.

Keywords

Haemonchus contortus, $GABA_A$ agonists, $GABA_A$ receptors, homology modeling, cys-loop receptors

Acknowledgements

I would like to thank my fellow graduate students for bearing with my insanity during those marathon sessions of electrophysiology. Your discussions around the water cooler were a necessary and welcomed distraction. I also want to thank past and present member of the Forrester lab for their support and collaboration. Micah, you helped make the lab a home away from home, may your recordings be ever clean and reproducible.

Of course I would also thank my family for all that they do.

Finally I would like to thank my supervisor Dr. Sean Forrester for mentoring me over the years. Your guidance and patience has been a constant inspiration and our discussions have broadened my understanding of the scientific world. Thank you very much.

Table of Contents

List of Tables

List of Figures

different from 500μM GABA alone ($P \leq 0.05$). Error bars represent SEM with n=4.

Figure 6: Effect of incorporating Hco-UNC-49C subunit(s) into the channel alters sensitivity profile of compounds. Dose-response curve of TACA is relative to a maximal GABA concentration. n>6.

Figure 7: (A) GABA molecule docked in the putative binding site. Side-chains of the residues that make up the aromatic box are labelled. Nitrogens and oxygens are labelled blue and red respectively (B) Hco-UNC-49B homodimer model. The discontinuous binding loops are highlighted in black and labelled.

Figure 8: Comparative docking of agonists into the binding site of Hco-UNC-49B. Shown are the residues (grey) of the defined aromatic box, with oxygens labelled red and nitrogens blue. Teal molecules in panels are: (A) β-alanine, (B) DAVA, (C) glycine, (D) TACA, (E) Et-4AB, (F) IMA, (G) (R)-(-)-GABOB, (H) (S)-(+)-AHBA, (I) GAA, (J) GPA, (K) isoguvacine, and (L) isonipecotic acid. Racemic mixtures of GABOB and AHBA were electrophysiologically tested, but binding orientations between enantiomers varied little. As such, only one enantiomer of each is shown.

List of Appendices

List of Abbreviations

3-APA → 3-aminopropylphosphonic acid

5-HT → Serotonin

$5\text{-}HT_3$ →Serotonin-gated ion channel

Ach → Acetylcholine

AChBP → Acetylcholine binding protein

AHBA →4-amino-2-hydroxybutyric acid

APMPA →3-aminopropyl(methyl)-phosphinic acid

Arg → Arginine

B → Fraction of agonist occupying a receptor

B_{max} → Maximum receptor occupancy

CNS → Central nervous system

cRNA → copy RNA

[D] → Concentration of agonist

DAVA → 5-aminovaleric acid

dSEVC → discontinuous single-electrode voltage clamp

DMSO → Dimethyl sulphoxide

EC50 → measure of potency and describes the concentration required for half maximum response

ECD → Extracellular domain

ELIC → *Erwinia* ligand-gated ion channel

Et-4AB → Ethyl-4-aminobutyrate

GAA → Guanidinoacetic acid

GABA → ɣ-aminobutyric acid

$GABA_A$ → Vertebrate GABA-gated chloride channel

$GABA_C$ → ρ-containing vertebrate GABA-gated chloride channel

Gabazine →6-Imino-3-(4-methoxyphenyl)-1(6*H*)-pyridazinebutanoic acid hydrobromide

GABOB → 4-amino-3-hydroxybutyric acid

GAD → Glutamic acid decarboxylase

GLIC → *Gloeobacter* ligand-gated ion channel

GlyR → Glycine-gated chloride channel

GPA → Guanidinopropionic acid

GRD →Glycine-like receptor

h → Hill slope

Hco-UNC-49B → *Haemonchus contortus* uncoordinated gene 49 homopentameric protein structure

Hco-UNC-49BC → *Haemonchus contortus* uncoordinated gene 49 heteropentameric protein structure

IMA → Imidazole-4-acetic acid

I_{max} → maximal current response of an agonist

K_d → Dissociation equilibrium rate constant

LCCH3 → ligand-gated chloride channel homologue 3

LGIC → Cys-looped ligand-gated ion channel

M1-4 → Transmembrane domains 1 through 4

MS-222 → 3-aminobenzoic acid ethyl ester methane sulphonate salt

n → Number of replicates

NMJ → Neuromuscular junction

nAchR → Nicotinic acetylcholine receptor

P4S → Piperidine-4-sulphonic acid

Phe →Phenylalanine

RDL →Resistant to dieldrin receptor

SCAM → Scanning cysteine accessibility mutagenesis

SEM → Standard error of the mean

TACA → trans-4-aminocrotonic acid

TEVC → two-electrode voltage clamp

Thr → Threonine

Tyr → Tyrosine

Chapter 1: Introduction

1.1 Cys-Loop Ligand-gated Ion Channels

Cys-loop ligand-gated ion channels (LGICs) are a family of pentameric, membrane-spanning, allosteric proteins that facilitate the movement of ions across a biological membrane. Members of this family are characterized by a conserved 13 amino acid loop in the N-terminal extracellular domain (ECD) formed from a disulphide bond between two cysteine residues (Ortells and Lunt, 1995). Interestingly, bacterial LGICs have been identified which lack this cys-loop feature. In place of the disulphide bond, prokaryote LGICs exhibit a conserved hydrophobic interaction to stabilize the region (Tasneem et al., 2004). Apart from the cys-loop, the large N-terminal ECD also contains the binding pocket located at the interface between two subunits (Brejc et al., 2001). Each subunit is composed of four transmembrane domains (M1-4), where M2 lines a central pore, around which the five subunits assemble (see Figure 1). This pore region energetically favors a closed conformation in the unoccupied resting state (Brejc et al., 2001; Kawate et al., 2009). Channel configurations can be homopentamers of a single subunit such as ρ-containing γ-aminobutyric acid (GABA) channels (Cutting et al., 1991) and ATP P2X receptors (Torres et al., 1999). However, *in vivo* receptor populations are more often a mix of different subunits (Lester et al., 2004).

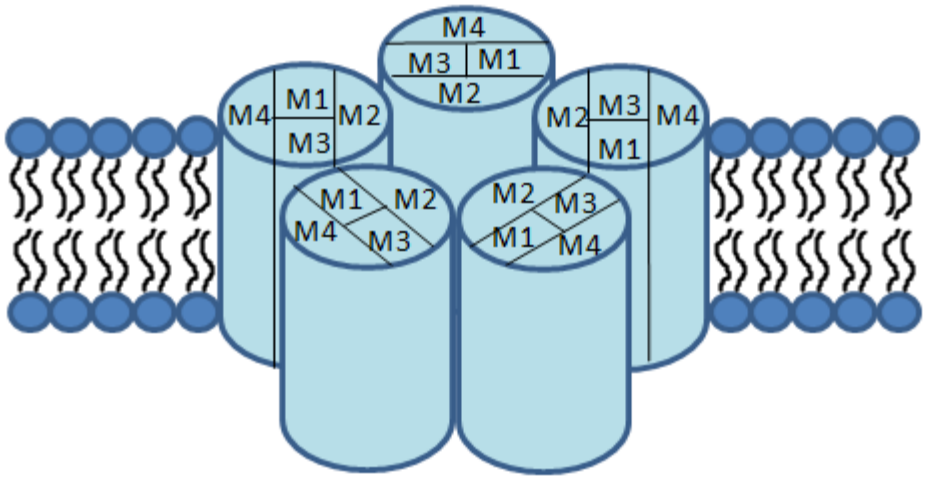

Figure 1: Assembly of a pentameric LGIC with the M2 domain lining the pore (Adapted from Moss and Smart, 2001).

Opening of the channel gate is facilitated by agonist binding. Neurotransmitters are the primary endogenous agonists of LGICs. These channels gate specific ions, and thus are categorized as either anion or cation selective. The major classes of cationic channels are excitatory and include the nicotinic acetylcholine receptor (nAchR) (Dani and Bertrand, 2006) and serotonin receptor (5-HT_3) (Reeves and Lummis, 2002). Inhibitory anionic LGICs include GABA ($GABA_A$) (Levitan et al., 1988), and glycine receptors (GlyR) (Langosch et al., 2005). LGICs are found extensively throughout the central nervous system (CNS) (Dani, 2001) and operate on the millisecond timescale (Stroud et al., 1990). Pre-synaptic cells release neurotransmitters to bind LGIC located on the post-synaptic cell propagating excitatory signals (from cations) or inhibitory signals (from anions). In this manner, LGICs facilitate fast synaptic neurotransmission.

1.1.1 The Binding Pocket

Binding of an agonist to the extracellular domain (ECD) increases the probability of the channel undergoing a conformational change, facilitating the opening of the "gate" of the pore and allowing ion passage. Much of our understanding of binding events stems from studies of X-ray crystallography, mutagenesis (Sigel et al., 1992; Wagner et al., 2004), photoaffinity-labelling (Smith and Olsen, 1994), and electrophysiological analysis (Bormann, 1988) (See Thompson et al., 2010 for further review). High resolution X-ray crystallography provides the best look at LGICs, but the nature of membrane protein work is prohibitively difficult, and as a result few crystal structures are available today. From the 2.7Å resolution crystal structure of the Acetylcholine binding protein (AChBP) of the snail *Lymnea stagnalis*, it was verified that the orthosteric binding of agonists occurs at the interface between two adjacent subunits (Brejc et al., 2001). AChBPs are homologous to the ligand binding domain of LGICs and are used extensively for homology modeling of LGICs whose crystal structure has yet to be determined (Sixma and Smit, 2003). More recent crystal structures of the ECD from prokaryote LGICs (Bocquet et al., 2009), and nAchR (Dellisanti et al., 2007), support the use of AChBP as a model and provides further evidence that the ligand binding site is situated between two adjacent subunits, the "principal" subunit and the "complimentary" subunit. These subunits contribute different residues to the binding event. In addition, a minimum of two activated binding sites are required for most channel opening (Thompson et al., 2010). Often an initial binding event creates a more favorable binding opportunity for

subsequent agonists, a phenomenon known as cooperative binding, as defined by the equation (Hill, 1910):

$$\log\left(\frac{B}{Bmax - B}\right) = h \cdot \log[D] - \log\mathrm{Kd}$$

Where B is the fraction of agonist occupancy, B_{max} is the maximum occupancy, D is the concentration of free ligand and K_d is the dissociation constant. A Hill slope, *h*, describes the slope of the dose-response curve. An *h* value greater than one suggests cooperative binding as seen with most LGIC agonists (Thompson et al., 2010).

The binding of agonists occurs in a specific pocket in the ECD that is rich in aromatic amino acids (Eiselé et al., 1993). One of the primary bonds that occur between the agonist and the binding pocket is a single, specific π-cation interaction. Here, the positively charged amine group of the agonist affiliates with the electronegative side-chain of an aromatic amino acid, often tryptophan (Zhong et al., 1998; Beene et al., 2002). Using unnatural amino acid mutagenesis, the polar ring of aromatic residues can be systematically fluorinated. This fluorination reduces the electronegativity of the ring, and thus reduces or eliminates the strength of the bond with agonists (Beene et al., 2003). If the aromatic residue in question is contributing to the π-cation bond, then increased fluorination should result in a reduced ability of agonists to bind and open the channel. Indeed, fluorination of tyrosine 198 (Tyr198) position of the $GABA_C$ receptor reduces the conductance of chloride ions compared to wildtype receptors (Lummis et al., 2005). Further evidence for π-cation interactions is provided from studies using homology models and loss of function mutations (Abdel-Halim et al., 2008).

The complete agonist binding site is formed from six discontinuous "Loop" regions contributed by both adjacent subunits. The principal subunit contributes Loops A-C while the complimentary subunit supplies Loops D-F (Figure 2). It is noteworthy that, although the relative position of the residue partaking in the π-cation bond differs from receptor to receptor, (Beene et al., 2002; Lummis et al., 2005; Padgett et al., 2007; Pless et al., 2008), the residues that contribute this bond have only been found on the principal subunit.

Figure 2: The six discontinuous Loops that make up the aromatic box. Shown above are two adjacent Hco-UNC-49B subunits with GABA positioned in the binding site. Adapted from Accardi and Forrester, (2011).

Simultaneous electrophysiological and radiolabelled binding studies using ^{3}H-labelled GABA indicate that agonist binding locks the molecule in place for the duration of channel opening (Cheng and Weiss, 1999). This bound state creates a stabilizing tightening of the binding pocket (i.e. closing) which is required for opening the channel (Armstrong and Gouaux, 2000; Hansen et al., 2005). Conversely, antagonists, which are

often bulkier than their agonist counterparts, bind but prevent the pocket from closing and therefore the channel gate remains closed (Armstrong and Gouaux, 2000; Hansen et al., 2005).

1.1.2 Linking Binding to Gating

The question of exactly how binding of an agonist opens the channel gate has plagued the field from its infancy, and is still not fully understood. Loss of function mutations of the cysteine-loop indicates its involvement in this process (Schofield et al., 2003). Another key component appears to involve the extracellular M2-M3 linker region, as identified by crystallography (Miyazawa et al., 2003) and scanning cysteine accessibility mutagenesis (SCAM) analysis. SCAM involves creating a functional cysteine-less mutant, then systematically mutating residues of interest into cysteine. Electrophysiology is carried out with the co-application of a sulphydryl reagent with either agonists or antagonists. If the mutated cysteine position experiences movement when the receptor binds to an agonist, it may affect its availability to bind to the sulphydryl reagents. Using SCAM, Bera et al. (2002) identified movement in the M2-M3 linker region to a more water accessible environment during gating. Site-directed mutagenesis of residues in the M2-M3 linker region has also been shown to affect gating (Campos-Caro et al., 1996; Kusama et al., 1994).

Du et al. (2012) summarizes how, using modeling (Zheng and Auerbach, 2011) and the Unwin model (Unwin et al., 2002), a binding event may distress local residues initiating a conformational wave passing through the cys-loop into the M2-M3 domain.

This destabilization likely involves rotation of the ECD, which forces the pore and gate-forming M2 domain to tilt outwards and open the gate.

1.1.3 The Pore

Studies assessing the amino acid composition of M2 have shown the presence of a kink within the M2 helix that has been identified as the gate structure (Unwin et al., 2005). It is the symmetrical outward tilting of the M2 domains which moves the kink and provides the space for ions to pass into the cell (Thompson et al., 2010). LGICs are capable of spontaneously opening without ligand binding, but this phenomenon is very rare and energetically unfavourable (Hu and Peoples, 2008). The amino acids that make up the narrowest section of the gate are composed of serine, threonine or valine depending on the channel type (Thomson et al., 2010). Certain mutations to this gate which reduce the size of the amino acid side-groups create constitutively active channels resulting, for the most part, in unregulated movement of ions (Pan et al., 1997). Main ion selectivity for conductance occurs at a membrane cross-section below the gate called the intermediate ring. This ring is composed of glutamic acid in cationic channels and uncharged residues in anionic channels (Wotring et al., 2003; Konno et al., 1991). Mutagenesis of these regions can actually switch ion selectivity of the channel (Keramidas et al., 2000).

1.2 Bacterial LGICs

LGICs have been identified across the animal kingdom and in prokaryotes. Cockcroft et al. (1990) hypothesized that LGICs originated before the dawn of eukaryotes. According to Cockcroft's tree, the origin of channel gating predates

eukaryote divergence, and likely early small molecules could bind and induce ion specific currents. A role of chemosensation in the single-celled organism might have created the evolutionary pathway that led to the neurotransmitter signal transduction seen today. At the more basic level of life, LGICs have been found to have a role in pH- and osmo-regulation (Stock et al., 1977).

The crystal structure of two bacterial LGICs, the *Erwinia* ligand-gated ion channel (ELIC), and the *Gloeobacter* ligand-gated ion channel (GLIC) have been solved and bear striking similarities with other LGICs (Hilf and Dutzler, 2008; Bocquet et al., 2009). Although these channels lack a cys-loop and an intracellular domain, they share the same pentameric structure as well as mechanism of binding and gating as other LGICs. ELIC is a cationic GABA-gated channel that is sensitive to similar open channel blockers as other LGICs (Thompson et al., 2012). This suggests a conserved pore region for this family of receptors. Interestingly, ELIC is sensitive to benzodiazepines, but not classic competitive orthosteric $GABA_A$ antagonists (Thompson et al., 2012), illustrating the fact that direct comparisons with other GABA receptors will have its limits.

1.3 Vertebrate GABA Receptors

There are two classes of vertebrate GABA receptors; $GABA_A$ type LGICs and $GABA_B$ type G protein coupled receptors (GPCRs) (Jones et al., 1998). GABA-gated LGICs are responsible for the majority of inhibitory signalling in the CNS. These channels are activated by the small amino-acid derivative GABA. GABA is formed through the actions of the glutamic acid decarboxylase enzyme (GAD) (Tappaz et al., 1977). GABA is then transported into vesicles found mostly on interneuron pre-synaptic

cells where it is released following an action potential (Freund and Buzsaki, 1996). The amount of neurotransmitter vesicle release is synchronized and operates in the millisecond timescale (Kraushaar and Jones, 2000).

1.3.1 $GABA_A$ Receptors

Unlike those of prokaryotes, LGICs such as $GABA_A$ receptors play a role in signal transmission. GABA is released from pre-synaptic vesicles upon electrical activation of the cell (Burgoyne and Barclay, 2002) whereby they migrate across a synapse to bind to receptors on the post-synaptic cell membrane, inducing hyperpolarization through the influx of chloride ions. $GABA_A$ channels are composed of eight classes of subunits (α1-6, β1-4, ɣ2, θ, δ, ε, π and ρ) with several exhibiting long and short splice variants (Simon et al., 2004). Functional $GABA_A$ receptors require the co-assembly of at least 2α, and 2β subunits (Barnard et al., 1998; Farrar et al., 1999), the most common form being composed of two α1, two β2, and one γ2 (Ernst et al., 2003; Benke et al., 2004). The ɣ2 subunit is required for benzodiazepine sensitivity (Pritchett et al., 1989). Different subunit arrangements will confer different pharmacological and electrophysiological properties (Sieghart, 1995).

The $GABA_A$ receptor binding site is composed of a conserved aromatic box which is made up of aromatic residues from four binding loops (Loop A: Tyr97; Loop B: Tyr157; Loop C: Tyr205; Loop D: Phe64) located at the interface of a principal β and a complimentary α subunit. The residue Tyr97 makes a π-cation interaction with the amine of GABA (Padgett et al., 2007). Other residues on the principal subunit required for binding include arginine 207 (Arg207), which may directly interact with the carboxyl

group of the GABA molecule (Wagner et al., 2004) and Tyr157 which may hydrogen bond with Thr130 from the α subunit to help stabilize the binding pocket. These interactions better enable GABA to bind and elicit the full conformational change to open the gate (Padgett et al., 2007).

1.3.2 GABAc Receptors

GABAc is a subclass of $GABA_A$ receptors composed entirely of ρ subunits (Olsen and Sieghart, 2008). Unlike other $GABA_A$ receptors, these form homomeric channels with the agonist binding site located at the interface of two homologous subunits (Zhang et al., 2001). $GABA_C$ receptors were originally identified within populations of $GABA_A$ receptors by their insensitivity to the plant alkaloid bicuculline, a $GABA_A$ specific antagonist (Drew and Johnston, 1992). Other pharmacological differences include insensitivity to steroid anaesthetics, as well as propofol, barbituates, and benzodiazepines (Chang-sheng et al., 2003). Intuitively, insensitivity to the latter two can likely be attributed to the lack of the $GABA_A$ ɣ subunit which is required for their binding. Apart from pharmacological differences, these receptors exhibit a uniquely longer mean open time, lower conductance, and lower rate of desensitization than other $GABA_A$ channels (Zhang et al., 2001; Wotring et al., 1999; Chebib, 2004). Three ρ subunits have been identified, with varying agonist and antagonist pharmacologies (Pan et al., 2006). This new ρ (or rho) designation was chosen to label the subunits because they were first discovered in rhodopsin containing retina cells (Polenzani, et al., 1991; Cutting et al., 1991). Although not as ubiquitous as other $GABA_A$ receptors, $GABA_C$ are also found throughout the CNS (Wegelium et al., 1998; Enz and Cutting, 1999).

1.4 Invertebrate GABA Receptors

Invertebrates also utilize GABA for their own wide array of analogous GABA-gated chloride channels which are targets of a number of pharmaceuticals and insecticides. However, these receptors have not been as well characterized as their vertebrate counterparts.

A number of insect GABA receptors subunits have been identified including the *Drosophila melanogaster* resistant to dieldrin receptor (RDL) (ffrench-Constant et al., 1991), the glycine-like receptor (GRD) (Harvey et al., 1994), and the ligand-gated chloride channel homologue 3 (LCCH3) (Hendersen et al., 1993). Nematode GABA channels include LGC-37 (Laughton et al., 1994), LGC-38 (Siddiqui et al., 2012), UNC-49 and the EXP-1 cationic channel (Beg and Jorgensen, 2003).

1.4.1 The RDL GABA Receptor

RDL is one of the most well studied invertebrate GABA receptors and is expressed throughout the fly CNS (Hoise et al., 1997). Isolated from *Drosophila*, RLD was identified by mutant *rdl* genes resistant to the pesticide dieldrin (ffrench-Constant et al., 1991). These receptors play a regulatory role in olfaction and olfaction memory. Reduced RDL expression results in enhanced, but unstable olfaction learning (Boumghar et al., 2012). Like $GABA_C$, RDL receptors are capable of forming homopentameric channels (ffrench-Constant et al., 1993) and are bicuculline resistant (Zhang et al., 1994). Homology modeling of RDL consistently places the positively charged nitrogen of various agonists between two aromatic amino acids (Mcgonigle and Lummis, 2010). Further investigation using unnatural amino acid mutagenesis identified both residues as

contributing to π-cation bonds with the ligand. This is the first reported aromatic box to contain two residues involved in π-cation interactions; specifically Phe206 of Loop B and Tyr254 of Loop C (Lummis et al., 2011).

1.4.2 *Ascaris* Muscle GABA Receptors

In the early 1960s, Del Castillo et al. observed the ability of GABA (Del Castillo et al., 1964), and the anthelmintic piperazine (Del Castillo et al., 1963) to inhibit contractile activity on the human parasitic roundworm *Ascaris lumbricoides* muscle preparations. Likewise, Holden-Dye et al. (1989), and Martin (1982) observed similar effects of GABA agonists on the muscle of the related pig parasitic roundworm *Ascaris suum*. However, the pharmacological profile of these muscle GABA receptors was clearly different to what had been traditionally observed for vertebrate $GABA_A$ receptors. Specifically, the GABA receptor agonist IMA exhibited full agonist ability, something unseen for vertebrate GABA receptors. In addition, the nematode GABA receptors were unresponsive to sulphonated agonists of $GABA_A$, as well as benzodiazepines (Holden-Dye et al., 1989). Furthermore, these receptors are more resistant to known vertebrate GABA receptor blockers picrotoxin, dieldrin and t-butylbicyclophosphorothionate (Holden-Dye et al., 1989). These observations suggested that the receptors in question were GABA receptors unlike those of $GABA_A$ or $GABA_C$.

1.4.3 The Nematode UNC-49 GABA Receptor

In a study by McIntire et al. (1993), uncoordinated gene 49 (*unc*-49) lack of function mutants produced a “shrinker” phenotype whereby the roundworm *Caenorhabditis elegans* would be unable to relax its somatic muscles. Antibody labelled

GABA studies on *C. elegans*, showed a pattern of UNC-49 presence in the somatic muscle along motor neurons, with only a small presence in the central nerve cluster near the head (Bamber et al., 1999). This anatomical distribution is quite different from the CNS localization of vertebrate $GABA_A$ receptors. At the neuromuscular junction (NMJ) UNC-49 acts to coordinate movement by relaxing muscles during locomotion, allowing for a sinusoidal, snake-like movement. *unc-49* encodes for three unique GABA receptor subunits. These subunits, UNC-49A, UNC-49B, and UNC-49C are produced from the alternative splicing of one *unc-49* gene, a common phenomenon seen in nematode ion channels (Bamber et al., 1999). The B subunit has been shown to be required for GABA binding and is localized to the NMJ, where it may co-assemble with the C subunit to form a functional channel (Bamber et al., 1999). This B subunit appears to be similar to RDL and the $GABA_C$ ρ subunit as it is also able to form homomeric channels (Deng et al., 1986). UNC-49A does not co-localize with B or C, nor is it detected in comparable concentrations *in vivo* (Bamber et al., 2005). Initial pharmacological studies have indicated that the GABA binding site in UNC-49 is distinct from classical mammalian $GABA_A$ receptors as the GABA receptor antagonist bicuculline shows little activity at the nematode receptor (Bamber et al., 2003).

Haemonchus contortus Hco-UNC-49 subunits show similar splicing and function as the *C. elegans* channel (Siddiqui et al., 2010). Electrophysiological studies revealed that Hco-UNC-49 is a GABA-gated chloride channel distinct from the previously known Cel-UNC-49 channel (Siddiqui et al., 2010). Specifically, the UNC-49C subunit appears to be a positive modulator of GABA sensitivity in the *H. contortus* channel, but is a negative modulator in the *C. elegans* channel. Homology modeling coupled with

mutagenesis studies identified residues of the aromatic box to be composed of Loop A: Phe106, Loop B:Tyr166, Loop C: Tyr218, and Loop D: Tyr64, of which either Tyr166 or Tyr218 could make a π-cation interaction with GABA (Accardi and Forrester 2011).

Because of the unique neuromuscular function and pharmacology of UNC-49, it is a very appealing receptor with respect to drug development. Selectivity and specificity are always a primary concern when targeting parasites while attempting to minimize side effects to the host. Therefore, a detailed understanding of the differences between the nematode GABA receptors and any host homologs may increase the chance of developing both safe and effective novel antiparasitic drugs.

1.5 *Haemonchus contortus*

Haemonchus contortus is a parasitic nematode of ruminants such as goat and sheep. Unlike the completely free-living nematode *Caenorhabditis elegans, H. contortus* has both parasitic and free living life stages. Breeding occurs within the sheep abomasum and once the eggs develop to the 11-26 celled stage, they are excreted by the host among the feces into the fields. Eggs hatch and proceed to develop into their L2 larvae stage while feeding off bacteria in the soil and feces (Veglia, 1915). L3 larvae reach the parasitic life stage and migrate to the tops of grazing vegetation to be ingested. Upon reaching the abomasum, the now L4 larvae burrow into the mucosal membrane, undergoing a final moulting to ultimately reside by the stomach epithelia where they feed and breed; reproduction occurs while feeding (Nikolaou and Gasser, 2006). A key anatomical difference between *H. contortus* and *C. elegans* is the presence of a modified

mouth containing a hollowed spear used to facilitate penetration of host blood vessels (Veglia, 1915).

These blood feeding parasites reside in the abomasum of ruminants, triggering such sequelae as anemia, emaciation, weakened immune system, and even death (Allonby and Urquhat, 1975). These conditions in turn cause poor productivity and place a large financial burden on the farming industry. Parasitic nematodes also infect plant crops and almost 50% of the human race; this is especially prevalent in developing countries due to poor quality drinking water, as seen by the high incidence of river blindness, a disease caused by the parasitic nematode *Onchocerca volvulus* (Osei-Atweneboana et al., 2007). As such, numerous anthelmintic drugs have been created to combat these financial and health burdens. The most successful antiparasitic drugs target ligand-gated ion channels (Geary, 2005). However, drug resistance has diminished the effectiveness of nearly all antiparasitic drugs (Beech et al., 2010).

1.6 The *Xenopus laevis* Expression System

Early work with oocytes of the African Clawed frog, *Xenopus laevis*, established their ability to properly translate injected exogenous mRNA into proteins (Gurdon et al., 1971). A number of studies including those on LGICs use *X. laevis* oocytes as an expression system for proteins. *X. laevis* oocytes do not express many endogenous ion channels, preventing cross-activation and lowering background noise (Dascal, 1987). The size of the oocyte permits the use of the two-electrode voltage clamp (TEVC) measuring technique, as opposed to the less accurate and noisy discontinuous single-electrode voltage clamp (dSEVC) (Sherman-Gold, 1993). Additionally, they are a robust cell capable of maintaining membrane integrity under the constant exposure to drugs and heat

from a microscope. Although the currents observed may not truly reflect those in the endogenous physiological setting, this system allows for comparing relative responses.

1.7 Objectives

UNC-49 is a GABA gated chloride channel found throughout the phylum nematoda (Accardi et al., 2012). This suggests that the receptor plays an essential role in the biology of free-living and more importantly, parasitic nematodes. Very little is known regarding its structural determinism for orthosteric binding of agonists, an avenue that is often manipulated to create new drug leads. Preliminary work with UNC-49 suggests that it does not fit into the category of any known GABA receptor. This thesis describes the results of a comprehensive analysis of the agonist pharmacology of the UNC-49 receptor from *H. contortus* which was complemented by *in silico* homology modeling and ligand-docking. Overall, UNC-49 possesses a unique agonist profile apart from other GABA receptors and results indicate that there is a size restriction for agonist binding. This study is important as it has provided new information on the nature of the binding site and the requirements for channel activation. This is not only valuable for understanding the differences in GABA receptors between parasitic nematodes and vertebrates, but may assist in the discovery of novel, potent, and highly specific molecules that could act as antiparasitic drugs.

Chapter 2: Materials and Methods

2.1 cRNA Synthesis

Complementary DNA of *Hco-unc-49b* (Genbank Accession #: EU939734.1) and *Hco-unc-49c* (Genbank Accession #: EU049602.1) were previously cloned into the expression vector PT7TS and stored in 50% w/v glycerol at -80°C. PT7TS contains flanking 5' and 3' untranslated regions coding for *X. laevis* β-globin to prevent degradation inside *X. laevis* oocyte cytosol (Dent et al., 1997). Approximately, 0.4-1µg of linearized plasmid was used for the T7 RNA polymerase mMESSAGE mMACHINE *in vitro* transcription kit from Ambion (Ambion, Austin, TX, USA). Briefly, RNA polymerase machinery from the T7 bacteriophage recognizes a promoter site on the linear template and transcribes sense RNA. Roughly 20µg of capped copy RNA (cRNA) yield was achieved per reaction. cRNA was deoxyribonuclease treated, precipitated using lithium chloride, and resuspended in nuclease free water.

2.2 *Xenopus laevis* Oocyte Isolation

Female *Xenopus laevis* frogs were obtained from NASCO and fed a diet of 1g NASCO frog brittle twice weekly (Nasco, Fort Atkinson, WI, USA). They were housed in a climate-controlled, light-cycled room with regular changes to the water. Frogs were anesthetized with 0.15% 3-aminobenzoic acid ethyl ester methane sulphonate salt (MS-222) (Sigma-Aldrich, Oakville, ON, CA), prior to surgical removal of a section of ovary. MS-222 was buffered with $NaHCO_3$ to pH 7 +/- 0.5. Ovarian lobes extracted were sectioned into pieces containing roughly 10-20 oocytes prior to a defolliculation treatment of 2mg/ml collagenase-II (Sigma-Aldrich) in oocyte Ringer's solution (82 mM

NaCl, 2 mM KCl, 1 mM $MgCl_2$, 5 mM HEPES pH 7.5 (Sigma-Aldrich)). Defolliculation took place at room temperature under light shaking for two hours. Collagenase was washed from the oocytes with ND96 solution (1.8 mM $CaCl_2$, 96 mM NaCl, 2 mM KCl, 1 mM $MgCl_2$, 5mM HEPES pH 7.5) and allowed one hour to recover at 18°C in supplemented ND96 (supplemented with 275µg/ml pyruvic acid sodium salt (Sigma-Aldrich) for a source of carbon energy and 100µg/ml of the antibiotic gentamycin (Sigma-Aldrich).

2.2.1 *Xenopus laevis* Oocyte Injections

Stage V and VI oocytes were selected for cytoplasmic injection of cRNA. Injections were carried out using a Drummond Nanoject II (Drummond Scientific Company, Broomhall, PA, USA) mounted on micromanipulators (World Precision Instruments, Inc., Sarasota, FL, USA). Roughly 25ng of cRNA was preferentially injected into the vegetal pole of selected oocytes. To form heteromeric channels, equal concentrations of *Hco-unc-49b* and *Hco-unc-49c* were mixed and injected into the oocytes. Negative control oocytes were injected with nuclease free water. Oocytes were stored in supplemented ND96 and allowed to recover and express the cRNA for 48 hours, with bi-daily changes of supplemented ND96 solution.

2.3 List of Compounds Tested and Their Preparations

4-amino-3-hydroxybutyric acid (GABOB), 4-amino-2-hydroxybutyric acid (AHBA) and ethyl-4-aminobutyrate (Et-4AB) were gifts from Dr. Jean-Paul Desaulniers (UOIT). Sodium salicylate was a gift from Dr. Ayush Kumar (UOIT). Isoguvacine hydrochloride was purchased from Torcris (Tocris Bioscience, Bristol, U.K). All other

compounds were purchased from Sigma-Aldrich. These are ɣ-aminobutyric acid (GABA), β-alanine, 5-aminovaleric acid (DAVA), imidazole-4-acetic acid (IMA), guanidinoacetic acid (GAA), isonipecotic acid, trans-4-aminocrotonic acid (TACA), guanidinopropionic acid (GPA), dopamine, acetylcholine (Ach), 3-aminopropylphosphonic acid (3-APA), glutamic acid, glycine, piperidine-4-sulphonic acid (P4S), and taurine (see figure 3) Initial millimolar stock concentrations were dissolved in non-supplemented ND96. Water insoluble compounds were dissolved in 100% dimethyl sulphoxide (DMSO). These include guanidinopropionic acid, and guanidinoacetic acid. For these solutions 0.1% DMSO was added to non-supplemented ND96 wash solution and used in electrophysiological recordings. Fresh working concentrations of compounds were prepared each week.

2.4 Electrophysiological Recordings

Channel activity was measured using the two-electrode voltage clamp (TEVC) technique, utilizing an Axoclamp900A amplifier (from Molecular Devices, Sunnyvale, CA, USA). Oocytes were pierced using two microelectrodes filled with 3M KCl (1-5MΩ resistance), connected to Axon Instruments headstages (from Molecular Devices) via Ag|AgCl wire. Borosilicate glass microelectrodes were created using a P-97 Flaming/Brown micropipette puller (Sutter Instruments Company, Novato, CA, USA). Oocytes' voltages were clamped at -60mV to measure changes in the current-resistance relationship induced by channel opening. Oocytes were exposed to various compounds using a gravitational flow system into an RC-1Z perfusion chamber (Warner Instruments Inc., Holliston, MA, USA). Non-supplemented ND96 was used to wash compounds from the oocytes once a maximal current response was achieved. Electrophysiological

tracings were digitized onto a PC using an Axon Instruments Digidata 1440 (from Molecular Devices), recorded and saved using the Clampex 10.2 software (from Molecular Devices), and analyzed using Clampfit 10.2 (from Molecular Devices).

2.5 Statistical Analysis

Full agonist dose-response curves were produced using Prism 5.0 (Graphpad Software, San Diego, CA, USA). Curves were generated using the equation from Prism's log(agonist) vs.normalized response -variable slope setting :

$$Imax = \frac{1}{1 + \left(\frac{EC50}{[D]}\right)^{\mathrm{h}}}$$

Where I_{max} is the maximal current response of the agonist, EC_{50} is the concentration of agonist that produces half maximal response, [D] is the concentration of agonist, and *h* is the Hill slope. Relative dose-response curves were generated by defining maximal response relative to that of GABAs max response.

Averaged EC_{50} and *h* values, along with their standard error of mean (SEM) were calculated from at least three replicate oocytes from two separate frogs. All bar graphs were created using Microsoft Excel 2010. Statistical analysis was performed using a student's t-test where indicated in order to determine significance ($P<0.05$).

2.6 Homology Modeling

AChBP was used as the template for the generation of a 3-D Hco-UNC-49B homodimer to illustrate the binding pocket located at the interface between two B subunits. The extracellular coding sequence of Hco-UNC-49B (Genbank accession #:

ACL14329) was aligned to the 2.7 Å resolution, HEPES bound AChBP, chain A subunit (Genbank accession #: P58154) (Protein Data Bank ID 1I9B), which is widely used for homology modeling. This alignment was achieved using the align2d code of MODELLER9.10 (Sali and Blundell, 1993), and the dimer was prepared from a doubled alignment of AChBP with Hco-UNC-49B. A total of 50 models were generated to compensate for the poor sequence homology, and the most energetically favorable model with the least number of restraint violations was chosen from the MODELLER output file. These violations were assessed by means of their DOPE and molpdf scores; Ramachandran plot analysis was performed to evaluate structural violations (Lovell et al., 2002). UCSF Chimera 1.6.1 was used for imaging the models and preparing them for docking ligands (Pettersen et al., 2004).

2.6.1 Computational Ligand Docking

Energetically reduced zwitterion ligands were obtained from the Zinc database: http://zinc.docking.org/ (Irwin et al., 2012). Only the zwitterion of the compound AHBA was created and energy reduced using the MM2 force field from ChemBio3D Ultra 12.0 software (CambridgeSoft, Cambridge, U.K). Analysis of ligand length and charge separation distance was performed using the Display Distance Measurement program of ChemBio3D Ultra 12.0. Docking of ligands into the Hco-UNC-49B dimer was achieved using UCSF DOCK 6.5. The binding site was defined by a 10 Å region including the aromatic residues Tyr64 Phe106, Tyr166 and Tyr218 using the default parameters of DOCK accessory programs sphgen, grid and dock6.

Chapter 3: Results

3.1 Pharmacological Profile of Hco-UNC-49

3.1.1 Full Agonists

Hco-UNC-49B and Hco-UNC-49C encoding subunits of cRNA were successfully injected and expressed into *Xenopus laevis* oocytes. Application of GABA upon oocytes injected with Hco-UNC-49B exhibited an EC_{50} of 75.57 ±5.63 whereas oocytes injected with a mix of Hco-UNC-49B and C exhibited an EC_{50} of 59.24 ±7.73. Current responses to GABA on Hco-UNC-49B and BC expressing oocytes were concentration-dependent and comparable to previous work in our lab (Accardi and Forrester, 2011; Sididiqui et al., 2010). Because of the intrinsic uncertainty surrounding actual subunit composition from injecting a mix of subunits, the formation of a population of heterogeneous heteropentameric channels was assessed by nature of current-responses distinct from that of the homomeric channels. Oocytes injected with water elicited no current responses to any compound within the concentration ranges used in this study.

Agonists

GABA

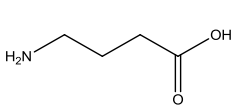

β-alanine

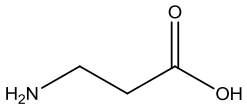

DAVA

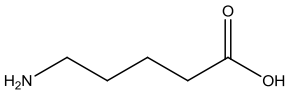

IMA

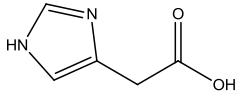

GABOB

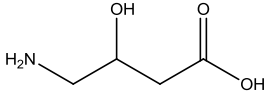

AHBA

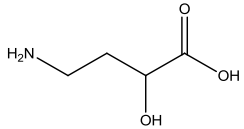

Isoguvacine

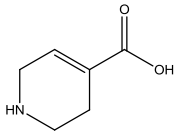

Isonipecotic acid

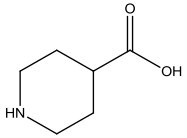

GAA

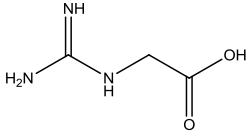

GPA

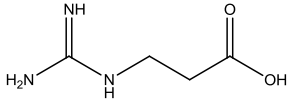

Et-4AB

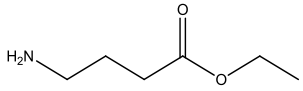

TACA

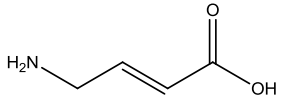

No Responses

3-APA

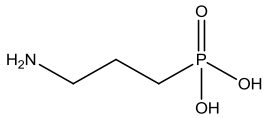

Glutamic acid

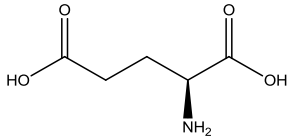

Glycine

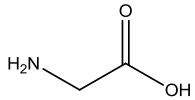

Taurine

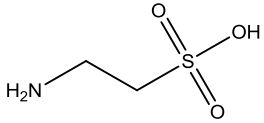

Ach

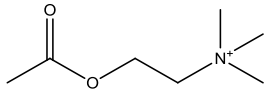

Sodium Salicylate

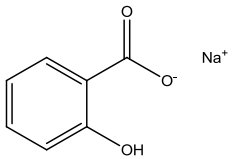

P4S

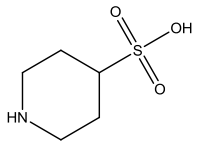

Dopamine

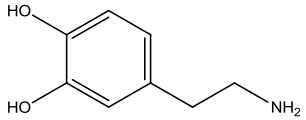

Figure 3: Chemical structure of the compounds assayed for agonist activity upon the Hco-UNC-49B and BC receptor complexes using TEVC. Compounds that activate Hco-UNC-49 are listed under Agonists, while those that elicited no current response are listed under No Responses

A pharmacological profile of Hco-UNC-49B and BC was performed against a range of compounds (Figure 3). These compounds were classically used $GABA_A$ agonists, or suspected to interact with the Hco-UNC-49 binding site based on chemical structure. Initial screening of each compound was performed at a minimum concentration of 500µM on three oocytes injected with *Hco-unc-49* and three water injected oocytes. In addition, each molecule was tested as an antagonist by co-applying 500µM of each compound with an EC_{50} concentration of GABA, and comparing this current to the current induced by GABA alone.

Of all the compounds tested, those that displayed no current responses (at the maximum concentration indicated) were glycine (5mM), taurine (5mM), sodium salicylate (5mM), Ach (5mM), P4S (5mM), 3-APA (500µM), dopamine (500µM), and glutamic acid (5mM).

Those compounds that displayed initial agonist activity were selected for further analysis by means of concentration response analysis. Shown in Figure 4 are the representative electrophysiological traces of several agonists and their resultant dose-response curves on the heteropentameric channel relative to a maximal GABA concentration. From these trials, the rank order potency for Hco-UNC-49BC was determined to be GABA > TACA > Isoguvacine >> IMA > GABOB > GAA >> Et-4AB > Isonipecotic acid > DAVA > β-alanine >> GPA > AHBA (Table 1). GPA (5mM) only achieved 6.5% of an EC_{50} concentration of GABA (data not shown). AHBA weakly and partially activated the channel at a maximal concentration of 100mM achieving 30% of maximal GABA response.

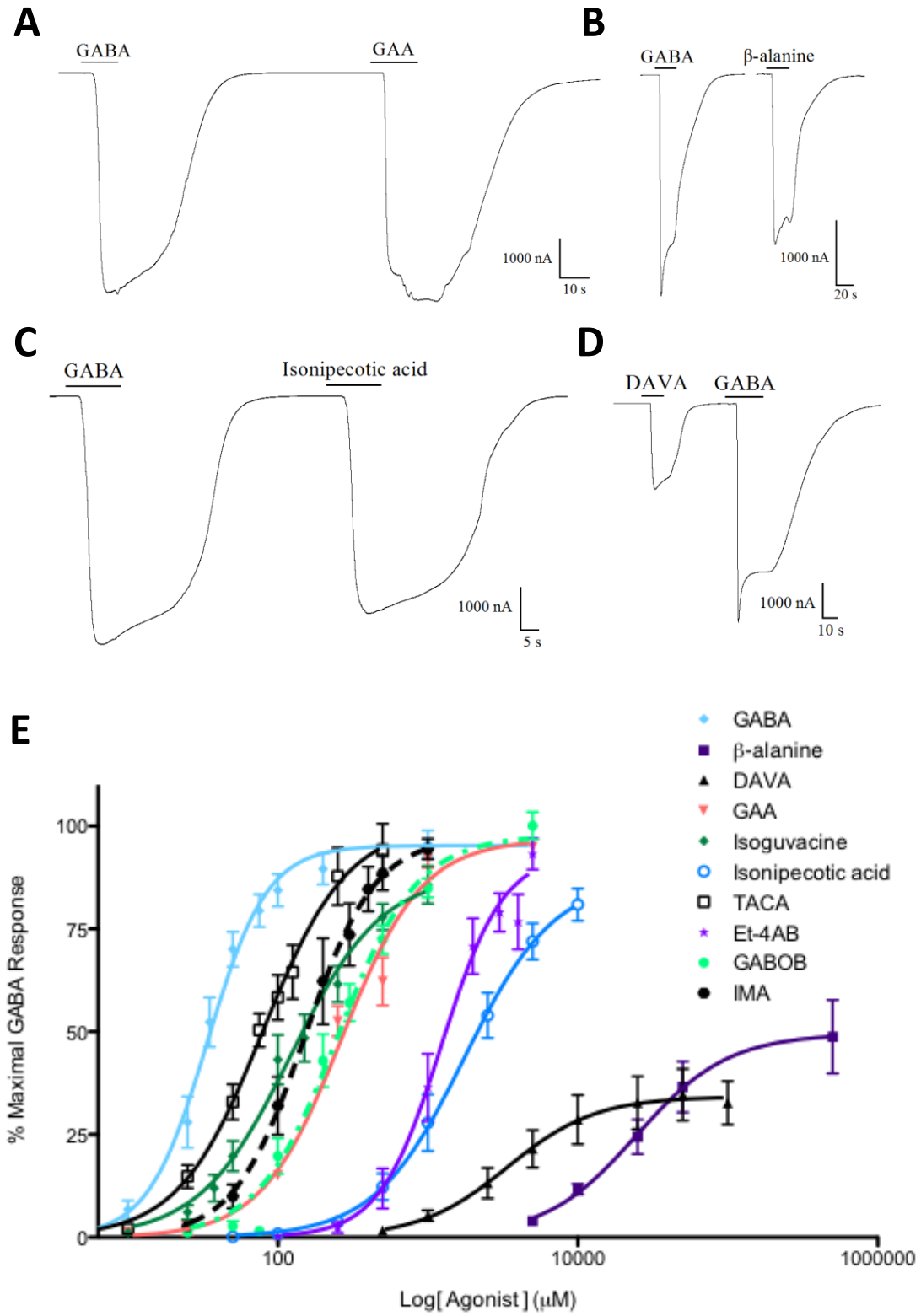

Figure 4: Comparative electrophysiological tracings comparing the maximal currents produced on the Hco-UNC-49BC receptor by 500μM GABA and (A) 10mM GAA (B) 500mM β-alanine (C) 10mM isonipecotic acid (D) 25mM DAVA. (E) Dose-response curves comparing agonist responses relative to maximal GABA; each datapoint is a mean ±SEM with n>3.

Table 1: EC_{50} and Hill slope values of agonists at the heteromeric and homomeric Hco-UNC-49 channels. Corresponding replicate numbers, n, and the ratio of heteromer:homomer EC_{50} values are included. Rank order potency is presented in descending order.

Compounds	**Hco-UNC-49BC EC_{50} ± SEM [µM] (*Hill slope ± SEM*)**	**n**	**Hco-UNC-49B EC_{50} ± SEM [µM] (*Hill slope ± SEM*)**	**n**	**BC/B**
GABA	**59.24 ±7.73** *(2.5 ±0.42)*	9	**75.57 ±5.63** *(2.62 ±0.12)*	7	.784
TACA	**78.15 ±5.23** *(2.25 ±0.33)*	11	**116.60 ±15.62** *(2.46 ±0.18)*	9	.67*
Isoguvacine	**99.29 ±11.87** *(1.95 ±0.3)*	14	**118.50 ±20.10** *(1.66 ± 0.19)*	11	.838
IMA	**174.53 ±20.75** *(1.93 ±0.17)*	11	**235.25 ±18.52** *(2.19 ±0.19)*	13	.742*
GABOB	**276.01 ±40.35** *(1.73 ±.075)*	7	**343.76 ±55.41** *(1.90 ±0.08)*	7	.803
GAA	**572.03 ±60.88** *(2.75 ± 0.05)*	3			
Et-4AB	**1268.40 ±173.82** *(2.4 ± 0.09)*	6	**1733.38 ±427.06** *(3.46 ±0.48)*	6	.732
Isonipecotic acid	**1725.25 ±362.03** *(1.78 ± 0.23)*	4			
DAVA[a]	**3914 ±520** *(1.47 ±0.18)*	7	**4350 ±290** *(1.47 ±0.12)*	7	.9
β-alanine[a]	**25 721 ±2806** *(1.49 ±0.19)*	7	**40 201 ±6166** *(1.50 ±0.1)*	6	.64*
GPA	-	6	-	6	-
AHBA[a]	-	3	-	3	-

[a] = Partial agonists
* = Statistically significant (P<0.05)

3.1.2 Partial Agonists

Interestingly, DAVA and β-alanine appear to be partial agonists with maximal responses of 32% and 49% respectively on the Hco-UNC-49BC channel. Further investigation of DAVA showed a characteristic partial agonist inhibitory effect of the GABA response. Specifically, at higher concentrations DAVA inhibited a maximal GABA induced current (Figure 5).

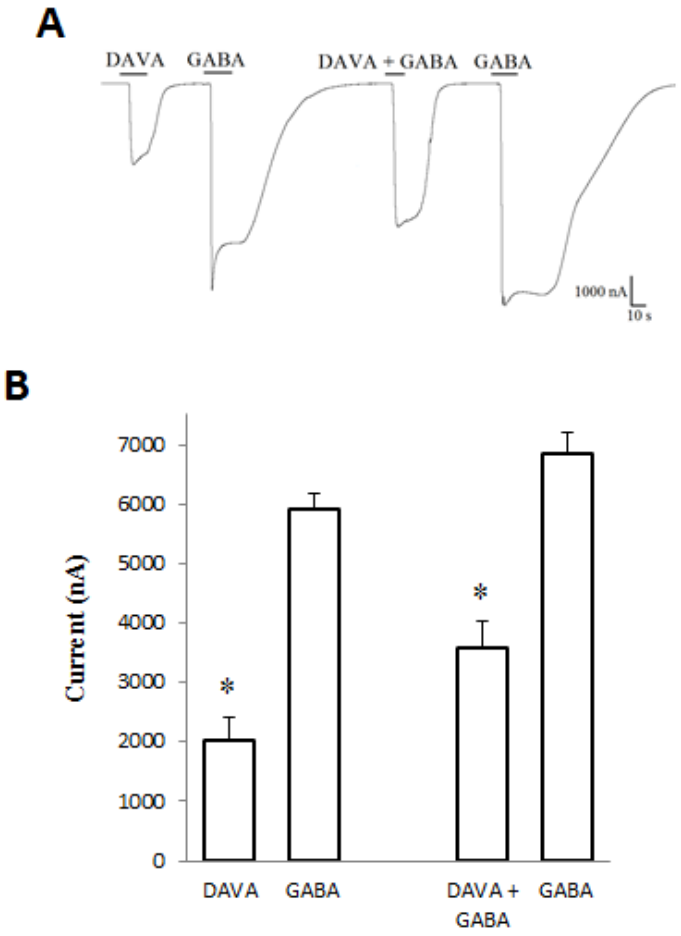

Figure 5: (A) Representative tracing showing the response of maximal DAVA (25mM), GABA (500µM) and the combination of 500µM GABA with 25mM of DAVA at the Hco-UNC-49BC channel. (B) Averaged current from 25mM DAVA, 500µM GABA, or both co-applied. Bars marked by (*) indicate current is significantly different from 500µM GABA alone ($P \leq 0.05$). Error bars represent SEM with n=4.

3.1.3 Comparison of Homomeric (B) and Heteromeric (BC) Channel Properties

As an additional confirmation of general trends in the efficacy of different agonists, the homomeric channel was also examined. As seen for the heteromeric channel, both DAVA and β-alanine also acted as partial agonists on the homomeric, Hco-UNC-49B channel. Both the homomeric and heteromeric channels share the same trends in their rank order potency for all the compounds examined in this study (Table 1). In addition, similar to their responses to GABA, the heteromeric channel generally exhibited a greater sensitivity to agonists compared to the homomeric channel. This increased sensitivity was often associated with a shift in EC_{50} (Figure 6; Table 1).

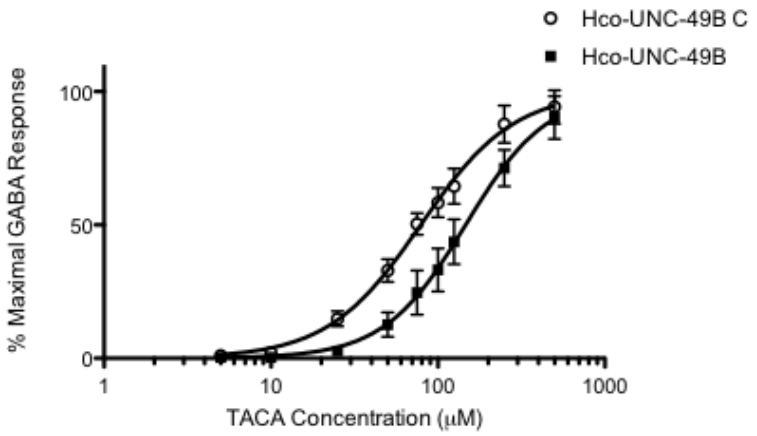

Figure 6: Effect of incorporating Hco-UNC-49C subunit(s) into the channel alters sensitivity profile of compounds. Dose-response curve of TACA is relative to a maximal GABA concentration. n>6

3.2 Homology Modeling and Docking

The AChBP (1I9B) was previously determined to be a suitable template for homology modeling of the Hco-UNC-49B extracellular domain, as described by Accardi and Forrester (2011). Figure 7 depicts the resulting homodimer with GABA docked into the binding pocket produced by homology modeling.

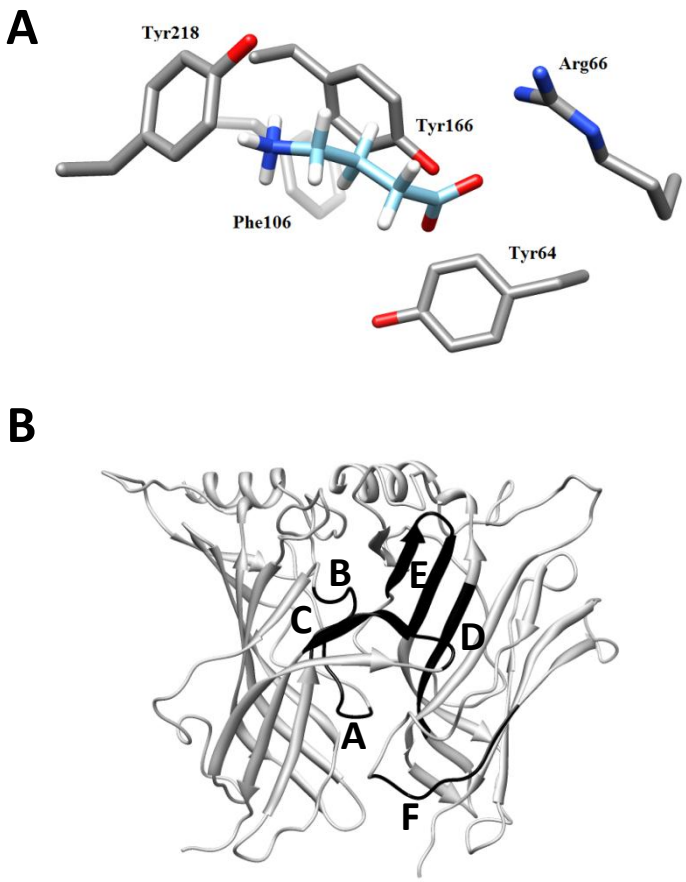

Figure 7: (A) GABA molecule docked in the putative binding site. Side-chains of the residues that make up the aromatic box are labelled. Nitrogens and oxygens are labelled blue and red respectively (B) Hco-UNC-49B homodimer model. The discontinuous binding loops are highlighted in black and labelled.

Invertebrate GABA receptors have been suggested to contribute two aromatic residues for π-cation interactions with ligands. Docking of GABA into the defined binding pocket aligns the amine group near the loop B Tyr166, as well as loop C Tyr218 (Figure 7). This is in accordance with a previous Hco-UNC-49B model (Accardi and Forrester, 2011). All agonists successfully docked within the defined 10 Å binding pocket, mostly orienting their amine group in the vicinity of Tyr166 and Tyr218 (Figure 8). Comparative docking of the agonists used in this study revealed differences in the orientations of the molecules within the binding site as well as the proximities of their respective amines with either of the tyrosine residues.

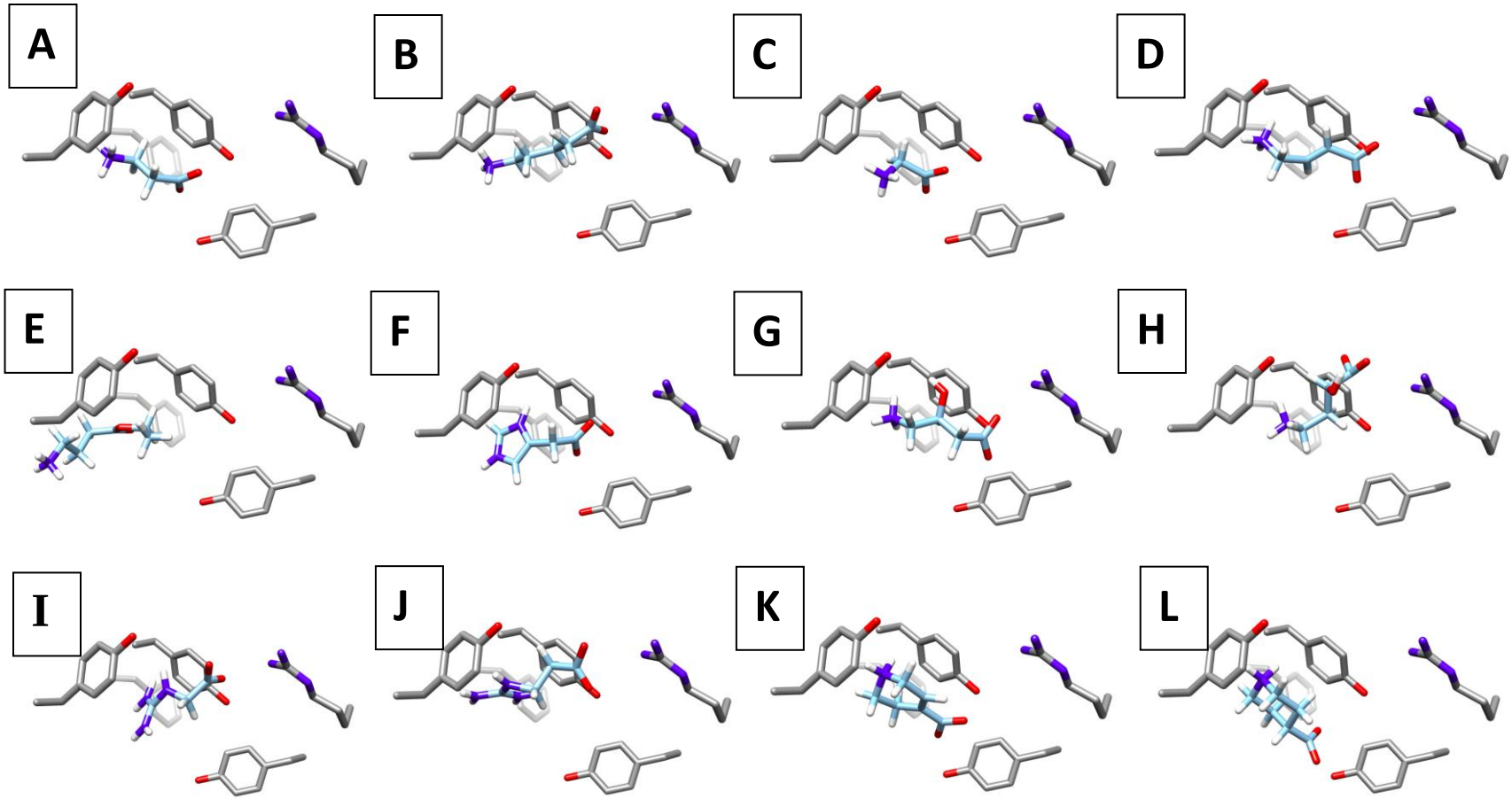

Figure 8: Comparative docking of agonists into the binding site of Hco-UNC-49B. Shown are the residues (grey) of the defined aromatic box, with oxygens labelled red and nitrogens blue. Teal molecules in panels are: (A) β-alanine, (B) DAVA, (C) glycine, (D) TACA, (E) Et-4AB, (F) IMA, (G) (R)-(-)-GABOB, (H) (S)-(+)-AHBA, (I) GAA, (J) GPA, (K) isoguvacine, and (L) isonipecotic acid. Racemic mixtures of GABOB and AHBA were electrophysiologically tested, but binding orientations between enantiomers varied little. As such, only one enantiomer of each is shown.

Glycine, β-alanine, GABOB, and TACA were all found to dock their amino groups in comparable fashion to that of GABA. Glycine and β-alanine carboxyl groups did not reach as deep into the binding cleft in comparison to GABA and TACA. Docking of DAVA positioned its amine group closer to Tyr218, tilting the carboxyl end away from the center of the cleft. AHBA and GABOB are two similar molecules with a hydroxyl group off the carbon backbone but at different positions. Because of this they dock with their carboxyl ends positioned in different orientations. Et-4AB was the largest compounds docked, with its ester group positioned closest to Tyr218 and Tyr166, pushing the amine group away from the pocket depths. IMA docked similarly to Et-4AB, except that its charged amine is located between Tyr218 and Tyr166. The carboxyl ends of GPA and GAA docked in the same position, but the charged amine of GAA was more equidistant between Tyr166 and Tyr218, whereas for GPA it was closer to Tyr218. Comparing isoguvacine and isonipecotic acid, it was their amine groups that docked in the same space, with the carboxyl of isonipecotic acid directed away from the binding pocket.

3.3 Molecular Measurements of Compounds

In order to rationalize the relationship between the electrophysiological EC_{50} values and the poses observed from docking, we measured the total atomic length and the distance between charged amine and carboxyl groups of the agonists (Table 2).

Table 2: Length measurements of docked charged agonists listing their relative potencies in descending order.

Ligand	Total molecule length (Å)	Dipole separation (Å)
GABA	6.9	6.1
TACA	6.6	5.7
Isoguvacine	5.9	4.9
IMA	6.6	5.6
GABOB	6.9	6.0
GAA	6.2	6.0
Et-4AB	10.3	6.1 [c]
Isonipecotic acid	5.9	4.9
DAVA[a]	8.1	7.3
β-alanine[a]	5.6	4.8
AHBA[a]	6.0	4.3
GPA	8.1	7.2
Glycine[b]	4.4	3.6

[a] = partial agonist
[b] = no response
[c] = no charged oxygen, distance measured for ether oxygen instead

Glycine is unable to elicit a current response on Hco-UNC-49, almost certainly a result of its small size. With one carbon longer than glycine, but one less than GABA, β-alanine is the shortest compound to activate the channel, and is a weak partial agonist. DAVA is also a weak partial agonist with one carbon different (longer) than GABA. GPA was the weakest partial agonist that generated a response and is one carbon longer than GAA (a full agonist). This difference increases the distance between charged groups by 1.2Å, identical to the difference seen between DAVA and GABA. The difference in hydroxyl positioning between GABOB and AHBA does not affect the molecular chain length, but causes the zwitterion of AHBA to curl up on itself, bringing the charged amine and carboxyl groups closer together than GABOB does. Isoguvacine and isonipecotic acid are the shortest full agonists and are identical in size. Unlike other GABA analogues, these

compounds contain bulkier ring structures in place of an amine group, which may affect binding. IMA is another cyclic compound, but is the same length as the straight chained TACA and both are full agonists. Et-4AB is a full agonist that is 2.1 Å longer than the partial agonist DAVA. It is also the only agonist that does not possess a charged carboxyl group. In place of a carboxyl group, Et-4AB contains a longer and uncharged ethyl ester.

Chapter 4: Discussion

4.1 Assessment of the Hco-UNC-49C Subunit

UNC-49 has been previously investigated regarding allosteric modulation and susceptibility to anthelmintics. However, little is known regarding agonist susceptibility. To address this deficiency, this thesis describes for the first time a pharmacological profile of a range of classical GABAeric compounds on both Hco-UNC-49B and Hco-UNC-49BC channels.

Hco-UNC-49 subunits expressed in *X. laevis* oocytes produced a population of dose responsive GABA-gated chloride channels eliciting currents similar to those previously studied in our lab (Siddiqui et al., 2010; Accardi and Forrester, 2011). These currents achieved microampere amplitude and were inhibited by the channel blocker picrotoxin and the allosteric modulator pregnenolone sulphate (Brown et al., 2011). The EC_{50} of GABA on the heteromer was 59.24 ±7.73μM, whilst 75.57 ±5.63 μM for the homomer. This tendency of the heteromeric channel to be more sensitive appears to be a trend for agonists at *H. contortus,* but not the *C. elegans* UNC-49 receptor (Siddiqui et al., 2010). Any difference in EC_{50}, Hill slope, or shape of the curve between the heteromer and homomer was attributed to the C subunit as its presence or absence is the only difference in preparing these oocytes. Previous research on both *H. contortus* and *C. elegans* UNC-49 receptors suggests that the C subunit appears to alter not only agonist, but allosteric modulator responses. When exposed to picrotoxin, UNC-49 channels containing C subunits appear to resist the blockage (Bamber et al., 2003; Brown et al., 2011). The role

of the C subunit may be limited to modulatory effects, analogous to $GABA_A$ γ subunit, which appears to be required for benzodiazepine binding (Pritchett et al., 1989).

4.2 Agonist Pharmacology

Based on structural analysis, it appears that there is a size restriction that dictates partial and full agonism in addition to potency (Table 2). This length-efficacy link is highlighted by glycine, β-alanine, GABA and DAVA, and is also suggested in a review by Du et al. (2012). An increase or decrease of a single carbon in the backbone of GABA prevents maximal channel activation and reduces potency by an order of magnitude. Comparing the docking of glycine, β-alanine, and DAVA to that of GABA into Hco-UNC-49B suggests an explanation to this phenomenon. Pless et al. (2011) showed that a number of GlyR agonists partake in a π-cation interaction with the same residue as glycine. In our study it appears that less efficacious compounds orient themselves further from the residues responsible for π-cation interactions, which likely reduces their ability to activate the channel.

In our model, a docked GABA molecule presents its amine group oriented almost equidistant between Tyr166 and Tyr218 of the principal subunit's Loop B and C respectively. Mutagenesis of both these residues caused over a 10-fold increase in EC_{50}, and both were suspected of participating in the π-cation bond with GABA (Accardi and Forrester, 2011). McGonigle and Lummis (2010) also observed the importance of those analogous residues in RDL, and suggested the possibility of two π-cation bonds. If this is the case for Hco-UNC-49 then agonists must approach both residues to fully open the channel. In support of this, DAVA and β-alanine both position their amine nearer to

Tyr218 than Tyr166 and fail to achieve maximal chloride conductance. Length also likely explains how GPA produces almost no response in comparison to the one carbon shorter GAA. This comparison is very similar to that of GABA and DAVA, which also exhibit a one carbon difference. GAA and GPA dock their carboxyl groups in a similar space, while the longer GPA places its amine group further from the two putative π-cation residues. Across from these putative π-cation contributing residues is an arginine that may bind the negatively charged carboxyl group of a ligand to stabilize the binding pocket. Mutation of the Hco-UNC-49B Arg66 yields channels with much reduced responses to GABA (Accardi and Forrester, 2011).This Arg-carboxyl association has been previously described for the GABA LGICs $GABA_A$ (Wagner et al., 2004), $GABA_C$ (Harrison and Lummis, 2006), and RDL (McGonigle and Lummis, 2010), as well as in the GlyR (Pless et al., 2011) suggesting a conserved role for this arginine residue. In our model GABA also docks with its carboxyl group positioned near Loop D's Arg66 of the complementary subunit. In comparison, the carboxyl of glycine and β-alanine fails to approach Arg66 as closely as GABA, due to their shorter length.

β-alanine, isonipecotic acid, and isoguvacine all have a dipole separation of 4.8-4.9 Å, yet β-alanine is the only partial agonist. The differences in potency could then be a result of the total size of the molecule. The cyclical compounds isoguvacine and isonipecotic acid are 0.3 Å longer and contain a bulkier piperidine in place of an amine group, allowing them to possibly wedge more fully into the binding crevice. The ~10 fold difference in efficacy between isoguvacine and isonipecotic acid has been previously observed for both vertebrate (Kusama et al., 1993) and invertebrate (Hoise and Sattelle, 1996) GABA receptors, and may be a result of the reduced planarness of isonipecotic

acid (Woodward et al., 1993) caused by the lack of a double bond in the ring. Docking shows that isoguvacine and isonipecotic bind with their amine groups in a similar space, but isonipecotic acid has its carboxyl group less directed towards Arg66, further suggesting the importance of an interaction with arginine. Whatever the cause, it is apparent that single changes to ligand structure can alter orientation of binding and effectiveness of gating. This may explain the drastic difference in efficacy between GABOB and AHBA. The 3-hydroxyl of GABOB permits full agonism while the 2-hydroxyl of AHBA yields a very weak partial agonist. It should be noted that regarding GABOB, we used a commercially available product composed of equal proportions R-(-)-GABOB and S-(+)-GABOB enantiomers. R-(-)-GABOB has been shown to be twice as potent as S-(+)-GABOB on both $GABA_A$ (Roberts et al., 1981) and $GABA_C$ (Hinton et al., 2008; Yamamoto et al., 2012a) receptors.

Contrary to the theme of size determinism, Et-4AB displayed full agonist properties. It should be noted that to the best of our knowledge Et-4AB has never been shown to be a GABA receptor agonist. Et-4AB is more than 2Å longer than the partial agonist DAVA, but displayed full agonist ability with a lower EC_{50}. Surprisingly, Et-4AB and DAVA dock in a similar orientation with the positively charged amine group pointed away from the binding site, which would reduce or eliminate any π-cation interactions. In addition, Et-4AB has no zwitterion state; the oxygen that normally ionizes is instead involved in the backbone of an ester. It is unclear whether Et-4AB participates in a π-cation bond without interacting with the Arg66, or if, contrary to our model the double bonded oxygen aligns with Arg66 and provides sufficient charge interaction to stabilize the binding pocket. Bower et al. (2008) has previously determined that various agonists of

the 5-HT_3 receptor do not necessarily interact with the same residues for channel activation. This may prove to be the case for a number of compounds investigated in this study, including Et-4AB.

4.3 Characterization Relative to Vertebrate GABA Receptors

There is now a sizable body of evidence suggesting a diversity of invertebrate and bacterial GABA-gated chloride channels that do not fall under the umbrella categorization of $GABA_A$ or $GABA_C$ type. However, in comparison to vertebrate GABA receptors, Hco-UNC-49 appears to follow more closely the agonist profile of the $GABA_A$ receptor. For example, GAA and DAVA both show antagonist properties on $GABA_C$, but were agonists of Hco-UNC-49BC and $GABA_A$ (Chebib et al., 2009; Kerr and Ong, 1995; Yamamoto et al., 2012b). Furthermore, isonipecotic acid only achieves partial agonist activity on the $GABA_C$, but is a full, albeit weak, agonist of UNC-49BC and $GABA_A$ (Kusama et al., 1993; Woodward et al., 1993). Deviating from this trend is the Hco-UNC-49 insensitivity towards sulphonated compounds such as taurine (del Olmo et al., 2000) and P4S which exhibit efficacy at the $GABA_A$ receptor but not $GABA_C$ (Woodward et al., 1993). Taken together, UNC-49BC channels exhibit a pharmacological profile separating themselves from those of their vertebrate analogues.

4.4 Characterization Relative to Invertebrate GABA Receptors

Martin (1982) showed that the application of the anthelmintic piperazine induced conductance of chloride ions into somatic muscle cells of the parasite *Ascaris suum*. From these early trials the pharmacological profile of the population of receptors found at the NMJ was assessed, but their identity was never elucidated. Table 3 compares the rank order potency of compounds tested from those muscle electrophysiology trials with another invertebrate GABA receptor (RDL) and the current study of the Hco-UNC-49 receptor.

Table 3: Rank order potencies of agonists on Hco-UNC-49BC, RDL, and *Ascaris suum* GABAergic receptors. Rank order potency is listed in descending order.

Hco-UNC-49BC	**RDL**[a]	**RDL**[b]	***Ascaris suum* Muscle**[c]
GABA	TACA	TACA	GABA
Muscimol[d]	GABA	GABA	TACA
TACA	Muscimol	Muscimol	R(-)GABOB
Isoguvacine	Isoguvacine	Isoguvacine	IMA
IMA	DAVA*	IMA	Muscimol
GABOB	β-alanine	Isonipecotic acid	Isoguvacine
GAA	P4S (Very weak)	β-alanine	S(+)GABOB
Et-4AB			GAA
Isonipecotic acid			DAVA
DAVA*			Isonipecotic acid
β-alanine*			
P4S (no response)			

* = partial agonist
[a] = from Mcgonigle and Lummis (2010)
[b] = from Hoise and Sattelle (1996)
[c] = from review: Martin (1993)
[d] = from Siddiqui et al. (2010)

Based on the physiological properties and pharmacological profiles, it appears that *A. suum* UNC-49 receptors might have been the primary ion channel investigated by Holden-Dye and Martin in the late 1980s. These receptors share the same anatomical distribution with Cel-UNC-49BC (Bamber et al., 2005), and a similar pharmacological profile with Hco-UNC-49. If UNC-49 is the receptor originally studied on the *Ascaris* muscle it is likely to be in the UNC-49BC configuration since both the *Ascaris* and UNC-49BC receptors are resistant to picrotoxin (Brown et al., 2011; Holden-dye et al., 1989; Bamber et al., 2003).

The *Drosophila* RDL receptor is another invertebrate channel that has garnered interest, with modeling and pharmacological profiles becoming increasingly prevalent. Independently, Hoise and Sattelle, (1996), and later Mcgonigle and Lummis, (2010) found a strikingly similar rank order potency of agonists that compares with Hco-UNC-49BC. A key difference between these receptors may be found in the size restriction of the binding pocket. One carbon shorter than GABA, β-alanine is a 10-fold more potent full agonist on RDL compared to being a weak partial agonist on Hco-UNC-49. On the other side, DAVA is one carbon longer than GABA and is a partial agonist with similar EC_{50} values for both the RDL receptor and Hco-UNC49. However, the maximal current responses of DAVA in the RDL receptor was ~75% of the GABA response compared to 32% in the Hco-UNC-49BC receptor. It is possible that the agonist binding site on Hco-UNC-49 has more stringent criteria for full activation.

4.5 Conclusion

This study characterized various agonist responses on the Hco-UNC-49 GABA gated chloride channel. Results of docking these agonists into a homology model of Hco-UNC-49B suggest that despite a variety of molecular sizes and functional groups, most agonists docked in a similar fashion within the aromatic box. The most potent of these agonists docked with their positively charged nitrogen group between Tyr166 and Tyr 218 and their negatively charged oxygen group near Arg66. Those agonists that failed to make these predicted interactions with local residues correlated with a weaker potency (higher EC_{50} value). Even small differences in functional group positioning or carbon backbone length were enough to severely impair potency. Comparing docking orientations of certain agonists such as the potent GAA and impotent GPA highlight this trend. The presence of an additional carbon in the backbone of GPA relative to GAA is associated with a slightly different binding orientation which equates to a drastic drop in potency. Future unnatural amino acid mutagenesis studies are required to verify the necessity of both Tyr166 and Tyr218 residues contributing π-cation interactions for channel activation. Also mutagenesis studies of the aromatic box coupled with competitive antagonist binding may shed further light on the importance of certain functional groups in determining agonist binding and gating.

The docking simulations described in this study assume that all agonists bind within the predicted binding cleft. However, this study did not investigate the possibility that certain agonists may bind to a site outside of this agonist binding site. For instance, the ability of Et-4AB to fully activate Hco-UNC-49 cannot be readily explained by conventional interactions with the aromatic box. Et-4AB docks its positively charged

nitrogen in a position suggestive of a partial agonist or even an inactive compound. In addition, the lack of a charged oxygen prevents an interaction with Arg66. Taken together with its docking orientation, the full agonist ability of Et-4AB implies unusual binding interactions.

Overall, the pharmacological profile described here exhibits similarity to previous studies of *Ascaris* muscle receptors. However, some differences were observed that are likely the result of differences in the cell type and species examined, and the assay used. However, overall the results from this thesis suggest that the previously characterized *Ascaris* GABA receptor was an UNC-49-like channel. If this is indeed the case then pharmaceutical targeting of UNC-49 may assist in a wide range of parasitic nematode infections.

Development of novel chemical controls for anthelmintics is essential for the continued prosperity of the agriculture sector. With climate change potentially increasing the rate of parasite infections coupled with human population growth, there is an urgent need for continued research on chemical control methods to cope with parasitic burdens. In order to continue producing selective drugs without harming the host, studies on the pharmacological profiles and the mechanisms behind binding and gating of novels targets are required. Results from this thesis provide further evidence that the agonist binding site of the UNC-49 receptor has a unique structure and sensitivity to various agonists and thus is a good candidate for both drug screening and rational drug design.

Chapter 5: References

Abdel-Halim, H., Hanrahan, JR., Hibbs, DE., Johnston, GAR., Chebib, M. 2008. A Molecular Basis for Agonist and Antagonist Actions at $GABA_C$ Receptors. *Chem Biol Drug Des*, 71:306-327.

Accardi, MV., Forrester, SG. 2011. The Haemonchus contortus UNC-49B subunit possesses the residues required for GABA sensitivity in homomeric and heteromeric channels. *Mol Biochem Parasit*, 178:15-22.

Accardi, MV., Beech, RN., Forrester, SG. 2012. Nematode cys-loop GABA receptors: biological function, pharmacology and sites of action for anthelmintics. *Invert Neurosci*, 12:3-12.

Allonby, EW., Urquhart, GM. 1975. The epidemiology and pathogenic significance of haemonchosis in amerino flock in East Africa. *Vet Parasitol*, 1:129-143.

Armstrong, N., Gouaux, E. 2000. Mechanisms for activation and antagonism of an APMA-sensitive glutamate receptor: crystal structures of the GluR2 ligand binding core. *Neuron*, 28:165-181.

Bamber, BA., Beg, AA., Twyman, RE., Jorgensen, EM. 1999. The *Caenorhabditis elegans unc-49* Locus Encodes Multiple Subunits of a Heteromultimeric GABA Receptor. *J Neurosci*, 19(13):5348-5359.

Bamber, BA., Twyman, RE., Jorgensen, EM. 2003. Pharmacological characterization of the homomeric and heteromeric UNC-49 GABA receptors in *C. elegans*. *Br J Pharmacol*, 138:883-893.

Bamber, BA., Richmond, JE., Otto, JF., Jorgensen, EM. 2005. The composition of the GABA receptor at the Caenorhabditis elegans neuromuscular junction. *Br J Pharmacol*, 144:502-509.

Barnard, EA., Skolnick, P., Olsen TW., Mohler, H., Sieghart, W., Biggio, G., Braestrup, C., Batesonm AN., Langer, SZ. 1998. Subtypes of gamma-aminobutyric acid A receptors: classification of the bases of subunit structure and receptor function. *Pharmacol Rev*, 50:291-313.

Beech, R., Levitt, N., Cambos, M., Zhou, S., Forrester, SG. 2010. Association of ion-channel genotype and macrocyclic lactone sensitivity traits in Haemonchus contortus. *Mol Biochem Parasit*, 171:74-80.

Beene, DL., Brandt, GS., Zhong, WG., Zacharias, NM., Lester, HA., Dougherty, DA. 2002. Cation-pi interactions in ligand recognition by serotonergic (5-

HT(3A)) and nicotinic acetylcholine receptors: the anomalous binding properties of nicotine. *Biochem*, 41:10262-10269.

Beene, DL., Dougherty, DA., Lester, HA. 2003. Unnatural amino acid mutagenesis in mapping ion channel function. *Curr Opin Neurobiol*, 13:264-270.

Beg, AA., Jorgensen, EM. 2003. EXP-1 is an excitatory GABA-gated cation channel. *Nat Neurosci*, 6:1145–1152

Benke, D., Fakitsas, P., Roggenmoser, C., Michel, C., Rudolph, U., Mohler, H. 2004. Analysis of the presence and abundance of $GABA_A$ receptors containing two different types of alpha subunits in murine brain using point-mutated alpha subunits. *J Biol Chem*, 279:43654-43660.

Bera, M., Chatav, M., Akabas, M. 2002. GABA(A) receptor M2-3 loop secondary structure and changes in accessibility during channel gating. *J Biol Chem*, 277:43002-43010.

Bocquet, N., Nury, H., Baaden, M., Le Poupon, C., Changeux, J-P., Delarue, M., Corringer, P-J. 2009. X-ray structure of a pentameric ligand-gated ion channel in an apparently open conformation. *Nature*, 457:111-114.

Bormann, J. 1988. Electrophysiology of GABAA and GABAB receptor subtypes. *Trends Neurosci*, 11(3):112-116.

Boumghar, K., Couret-Fauvel, T., Garcia, M., Armengaud, C. 2012. Evidence for a role of GABA- and glutamate-gated chloride channels in olfactory memory. *Pharmacol Biochem Behaviour*, 103:69-75.

Bower, KS., Price, KL., Sturdee, LEC., Dayrell, M., Dougherty, DA. 2008. 5-Fluorotryptamine is a partial agonist at 5-HT_3 receptors, and reveals that size and electronegativity at the 5 position of tryptamine are critical for efficient receptor function. *Euro J Pharmacol*, 580(3):291-297.

Brejc, K., van Dijk, WJ., Klaassen, RV., Schuurmans, M., van der Oost, J., Smit, AB., Sixma, TK. 2001. Crystal structure of an Ach-binding protein reveals the ligand-binding domain of nicotinic receptors. *Nature*, 411:269-276.

Brown, DDR., Siddiqui, SZ., Kaji, MD., Forrester, SGF. 2011. Pharmacological characterization of the Haemonchus contortus GABA-gated chloride channel, Hco-UNC-49: Modulation by macrocyclic lactone anthelmintics and a receptor for piperazine. *Vet Parasit*, 185:201-209.

Burgoyne, RD., Barclay, JW. 2002. Splitting the quantum: regulation of quantal release during vesicle fusion. *Trends Neurosci*, 25(4):176-178.

Campos-Caro, A., Sala, S., Ballesta, JJ., Vicente-Agullo, F., Criado, M., Sala, F. 1996. A single residue in the M2-M3 loop is a major determinant of coupling between binding and gating in neuronal nicotinic receptors. *Pro Natl Acad Sci USA*, 93:6118-6123.

Chebib, M. 2004. GABAC receptor ion channels. *Clin Exp Pharmacol Physiol*, 31:800-804.

Chebib, M., Gavande, N., Wong, KW., Park, A., Premoli, I., Mewett, KN., Allan, RD., Duke, RK., Johnston, GAR., Hanrahan, JR. 2009. Guanidino Acids Act as ρ1 $GABA_C$ Receptor Antagonists. *Neurochem Res*, 34:1704-1711.

Chang-sheng, CS., Olcese, R., Olsen, RW. 2003. A single M1 Residue in the beta2 subunit alters channel gating of $GABA_A$ receptor in anaesthetic modulation and direct activation. *J Biol Chem*, 278:42821-42828.

Cheng, Y., Weiss, DS. 1999. Channel opening locks agonists onto the $GABA_C$ receptor. *Nature Neurosci*, 2(3):219-225.

Cockcroft, VB., Osguthorpe, DJ., Banard, EA., Friday, AE., Lunt, GG. 1990. Ligand-Gated Ion Channels Homology and Diversity. *Mol Neurobiol*, 4:129-169.

Cutting, GR., Lu, L., O'Hara, BF., Kasch, LM., Montrose-Rafizadeh, C., Donovan, DM., Shimada, S., Antonarakis, SE., Guggino, WB., Uhl, GR. 1991. Cloning of the gamma-aminobutyric acid (GABA) rho 1 cDNA: a GABA receptor subunit highly expressed in the retina. *Proc Natl Acad Sci USA*, 88(7):2673-2677.

Dani, JA. 2001. Overview of nicotinic receptors and their roles in the central nervous system. *Biol Psychiatry*, 49(3):166-174.

Dani, JA., Bertrand, D. 2006. Nicotinic acetylcholine receptors and nicotinic cholinergic mechanisms of the central nervous system. *Ann Rev Pharmacol Toxicol*, 47:699-729.

Dascal, N. 1987. The use of Xenopus oocytes for the study of ion channels. *Crit Rev Biochem*, 22(4):317-387.

del Olmo, N., Bustamante, J., Solis., JM. 2000. Taurine activates GABA(A) but not GABA(B) receptors in rat hippocampal CA1 area. *Brain Res*, 864(2):298-307.

Del Castillo, J., Morales, T., Sanchez, V. 1963. Action of piperazine on the neuromuscular system of Ascaris lumbricoides. *Nature*, 200:706-707.

Del Castilo, J., De Mello, WC., Morales, TA. 1964. Inhibitory action of gamma-aminobutyric acid (GABA) on Ascaris muscle, *Cellular Mol Life Sci*, 10:141-143.

Dellisanti, CD., Yao, Y., Stroud, JC., Wang, Z-Z., Chen, L. 2007. Crystal structure of the extracellular domain of nAChR α1 bound to α-bungarotoxin at 1.94 Å resolution. *Nature Neorosci*, 10:953-962.

Deng L, Ransom WR, Olsen RW. 1986. [3H]Muscimol photolabels the γ-aminobutyric acid receptor binding site on a peptide subunit distinct from that labeled with benzodiazepines. *Biochem Biophys Res Commun,* 138:1308-1314

Dent, JA., Davis, MW., Avery, L. 1997. avr-15 encodes a chloride channel subunit that mediates inhibitory glutamatergic neurotransmission and ivermectin sensitivity in *Caenorhabditis elegans*. *EMBO J,* 16:5867–79.

Drew, CA., Johnston, GAR. 1992. Bicuculline- and baclofen-insensitive gamma-aminobutyric acid binding to rat cerebellar membranes. *J Neurochem*, 50:1087-1092.

Du, J., Dong, H., Zhou, H-X. 2012. Size matters in activation/inhibition of ligand-gated ion channels. *Trends Pharmacol Sci,* 33(9):482-493.

Eiselé, J-L., Bertrand, S., Galzi, J-L., Devillers-Thiéry, A., Changeux, J-P., Bertrand, D.1993. Chimaeric nicotinic-serotonergic receptor combines distinct ligand binding and channel Specificities. *Nature,* 366:479:483.

Enz, R., Cutting, GR. 1999. GABAC receptor rho subunits are heterogeneously expressed in the human CNS and form homo-and hetero-oligomers with distinct physical properties. *Eur J Neursci,* 11:42-50.

Ernst, M., Brauchart, D., Boresch, S., Sieghart, W. 2003. Comparative modeling of $GABA_A$ receptors: limits, insights, future developments. *J Neurosci*, 4:933-943.

Farrar, SJ., Whiting, PJ., Bonnert, TP., McKernan, RM. 1999. Stoichiometry of a ligand- gated ion channel determined by fluorescence energy transfer. *J Biol Chem*, 274:10100-10104.

ffrench-Constant, RH., Mortlock, PD., Shaffer, CD., MacIntyre, RJ., Roush, RT. 1991. Molecular cloning and transformation of cyclodiene resistance in *Drosophila*: An invertebrate gamma-aminobutyric acid subtype A receptor locus. *Proc Natl Acad Sci USA*, 88:7209-7213.

ffrench-Constant, RH., Rocheleau, TA., Steichen, JC., Chalmers, AE. 1993. A point mutation in a *Drosophila* GABA receptor confers insecticide resistance. *Nature*, 363:449-451.

Freund, TF., Buzsaki, G. 1996. Interneurons of the hippocampus. *Hippocampus*, 6:347-470.

Geary, TG. 2005. Ivermectin 20 years on: maturation of a wonder drug. *Trends Parasitol*, 21:530-532,

Gurdon, J **B., Lane, C.D., Woodland, H.R., Marbaix, G**. 1971. Use of frog eggs and oocytes for the study of messenger RNA and its translation in living cells. *Nature*, 233:177–182.

Hansen, SB., Sulzenbacher, G., Huxford, G., Marchot, P., Taylor, P., Bourne, Y. 2005. Structures of *Aplysia* AChBP complexes with nicotinic agonists and antagonists reveal distinctive binding interfaces and conformations. *EMBO J*, 24:3635-3646.

Harvey, RJ., Schmitt, B., Hermans-Borgmeyer, I., Gundelfinger, ED., Betz, H., Darlison, MG. 1994. Sequence of a *Drosophila* ligand-gated ion-channel polypeptide with an unusual amino-terminal extraceullular domain. *J Neurochem*, 62:2480-2483.

Harrison, NJ., Lummis, SCR. 2006. Locating the Carboxylate Group in the Homomeric rho $GABA_A$ Receptor Ligand-binding Pocket. *J Biol Chem*, 281(34):24455-24461.

Hendersen, JE., Soderlund, DM., Knipple, DC. 1993. Characterization of a putative gamma-aminobutyric acid (GABA) receptor beta subunit gene from *Drosophila melanogaster*. *Biochem Biophys Res Commun*, 193:474-482.

Hilf, RJ., Dutzler, R. 2008. X-ray structure of a prokaryotic pentameric ligand-gated ion channel. *Nature*, 452:375-379.

Hill, AV. 1910. The possible effects of the aggregation of the molecules of haemoglobin on its dissociation curves. *J Physiol*, 40(Suppl):iv-vii.

Hinton, T., Chebib, M., Johnston, GAR. 2008. Enantioselective action of 4-amino-3-hydroxybutanoic acid and (3-amino-2-hydroxypropyl)methylphosphinic acid at recombinant GABAc receptors. *Bioorg Med Chem Lett*, 18:402-404.

Hoise, AM., Sattelle, DB. 1996. Agonist pharmacology of two *Drosophila* GABA receptor splice variants. *Br J Pharmacol*, 119:1577-1585.

Hoise, AM., Aronstein, K., Sattelle, DB., Ffrench-Constant, RH. 1997. Molecular biology of insect neuronal GABA receptors. *Trends Neurosci*, 20:578-583.

Holden-Dye, L., Krogsgaard-Larsen, P., Nielsen, L., Walker, RJ. 1989. GABA receptors on the somatic muscle cells of the parasitic nematode, *Ascaris suum*:

stereoselectivity indicates similarity to a $GABA_A$-type agonist recognition site. *Br J Pharmacol*, 98:841- 850.

Hu, X-Q., Peoples, RW. 2008. The 5-HT(3B) Subunit confers spontaneous channel opening and altered ligand properties of the 5-HT3 receptor. *J Biol Chem*, 283(11):6826-6831.

Irwin, JJ., Sterling, T., Mysinger, MM., Bolstad, ES., Coleman, RG. 2012. ZINC: A Free Tool to Discover Chemistry for Biology. *J Chem Inf Model*, 52(7):1757-1768.

Jones, KA., Borowsky, B., Tamm, JA., Craig, DA., Durkin, MM., Dai, M., Yao, WJ., Johnson, M., Gunwaldensen, C., Huang, LY., Tang, C., Shen, Q., Salon, JA., Morse, J., Laz, T., Smith, KE., Nagarathnam, D., Nobel, SA., Brancheck, TA., Gerald, C. 1998. GABA(B) receptors function as a heteromeric assembly of the subunits GAABA(B)R1 and GABA(B)R2. *Nature*, 396:647-679.

Kawate, T., Michel, JC., Birdsong, WT., Gouaux, E. 2009. Crystal structure of the ATP-gated P2X4 in channel in the closed state. *Nature*, 460:592-598.

Keramidas, A., Moorhouse, AJ., French, CR., Schofield, PR., Barry, PH. 2000. M2 pore mutations convert the glycine receptor channel from being anion- to cation-selective. *Biophys J*, 79(1):247-259.

Kerr, DIB., Ong, J. 1995. $GABA_B$ RECEPTORS. *Pharmac Ther*, 67(2):187-246.

Konno, T., Musch, C., Von Kitzing, E., Imoto, K., Wang, F., Nakai, J., Mishina, M., Numa, S., Sakmann, B. 1991. Rings of anionic amino acids as structural determinants of ion selectivity in the acetylcholine receptor channel. *Proc R Soc Lond B Biol Sci*, 244:69-79.

Kraushaar, U., Jones, P. 2000. Efficacy and stability of quantal GABA release at a Hippocampal interneuron-principal of neuron synapse. *J Neurisc*, 20(15):5594-5607.

Kusama, T., Spivak, CE., Whiting, P., Dawson, VL., Schaeffer, JC., Uhl, GR. 1993. Pharmacology of GABA ρ1 and GABA α/β receptors expressed in *Xenopus* oocytes and COS cells. *Br J Pharmacol*, 109:200-206.

Kusama, T., Wang, JB., Spivak, CE., Uhl, GR. 1994. Mutagenesis of the GABA rho1 receptor alters agonist affinity and channel gating. *Neuroreport*, 5:1209-1212.

Langosch, D., Becker, C., Betz, H. 2005. The inhibitory glycine receptor: A ligand-gated chloride channel of the central nervous system. *Eu J Biochem*, 194:1-8.

Laughton, DL., Amar, M., Thomas, P.,Towner, P., Harris, P., Lunt, GG., Wolstenholme, AJ. 1994. Cloning of a putative inhibitory amino acid receptor subunit from the parasitic nematode Haemonchus contortus. *Recept Channels*, 2:155-63.

Lester, HA., Dibas, MI., Dahan, DS., Leite, JF., Dougherty, DA. 2004. Cys-loop receptors: new twists and turns. *Trends Neurosci*, 27(6):329-336.

Levitan, ES., Schofield, PR., Burt,DR., Rhee, LM., Wisden, W., Köhler, M., Fujita, N., Rodriguez, HF., Stephenson, A., Darlison, MG., Barnard, EA., Seeburg, PH. 1988. Structural and functional basis for $GABA_A$ receptor heterogeneity. *Nature*, 335:76-79.

Lovell, SC., Davis, IW., Arendall III WB., de Bakker, PIW., Word, JM., Prisant, MG., Richardson, DC. 2002. Structure validation by Calpha geometry: phi,psi and Cbeta deviation. *Proteins*, 50:437-450.

Lummis, SCR., Beene, DL., Harrison, NJ., Lester, HA., Dougherty, DA. 2005. A Cation-pi Binding Interaction with a Tyrosine in the Binding Site of the $GABA_C$ Receptor. C*hem Biol*, 12:993-997.

Lummis, SCR., McGonigle, I., Ashby, JA., Dougherty, DA. 2011. Two Amino Acid Residues Contribute to a Cation-pi Binding Interaction in the Binding Site of an Insect GABA Receptor. *J Neurosci*, 31(34):12371-12376.

Martin, RJ., 1982. Electrophysiological effects of piperazine and diethylcarbamazine on *Ascaris suum* somatic muscle. *Br J Pharmacol*, 77:255-265.

Martin, RJ., 1993. Neuromuscular transmission in nematode parasites and antinematodal drug action. *Pharmac Ther*, 58:13-50.

McGonigle, I., Lummis, SCR. 2010. Molecular Characterization of Agonists That Bind to an Insect GABA Receptor. *Biochem*, 49:2897-2902.

McIntire, SL., Jorgensen, E., Kaplan, J., Horvitz, HR. 1993. The GABAergic nervous system of Caenorhabditis elegans. *Nature*, 364:337-341.

Miyazawa, A., Fujiyoshi, Y., Unwin, N. 2003. Structure and gating mechanism of the acetylcholine receptor pore. *Nature*, 423:949-955.

Moss, SJ., Smart, TG. 2001. Constructing inhibitory synapses. *Nat Rev Neurosci*, 2:240-250.

Nikolaou, S., Gasser, RB. 2006. Prospects for exploring molecular developmental processes in *Haemonchus contortus. Int J Parasitol*, 36:859-868.

Olsen, RW., Sieghart, W. 2008. International union of pharmacology: LXX. Subtypes of gamma-aminobutyric acid(A) receptors: classification on the basis of subunit composition, pharmacology, and function. Update., *Pharmacol Rev,* 60(3):243-260.

Ortells, MO., Lunt, GG. 1995. Evolutionary history of the ligand-gated ion-channel superfamily of receptors. *Trends Neurosci*, 18:121-127.

Osei-Atweneboana, MY., Eng, JKL., Boakye, DA., Gyapong, JO., Prichard, RK. 2007. Prevalence and intensity of Onchocerca volvulus infection and efficacy of ivermectin in endemic communities in Ghana: a two-phase epidemiological study *Lancet*, 369:2021-2029.

Padgett, CL., Hanek, AP., Lester, HA., Dougherty, DA., Lummis, SCR. 2007. Unnatural Amino Acid Mutagenesis of the $GABA_A$ Receptor Binding Site Residues Reveals a Novel Cation-pi Interaction between GABA and beta2 Tyr97. *J Neurosci*, 24(4):886-892.

Pan, ZH., Zhang, D., Zhang, X., Lipton, SA. 1997. Agonist-induced closure of constitutively open gamma-aminobutyric acid channels with mutated M2 domains. *ProcNat Acad Sci USA*, 94:6490-6495.

Pan, Y., Ripps, H., Qian, H. 2006. Random Assembly of GABA ρ1 and ρ2 Subunits in the Formation of Heteromeric $GABA_C$ Receptors. Cellular and Molecular *Neurobiology*, 26(3):289-305.

Pettersen, EF., Goddard, TD., Huang, CC., Couch, GS., Greenblatt, DM., Meng, EC., Ferrin, TE. 2004. UCSF Chimera – a visualization system for exploratory research and analysis. *J Comput Chem*, 25:1605–12.

Pless, SA., Millen, KS., Hanek, AP., Lynch, JW., Lester, HA., Lummis SCR., Dougherty, DA. 2008. A cation-pi interaction in the binding site of the glycine receptor is mediated by a phenylalanine residue. *J Neurosci*, 28(43):10937-10942.

Pless, SA., Hanek, AP., Price, KL., Lynch, JW., Lester, HA., Dougherty, DA., Lummis, SCR. 2011. A Cation-pi Interaction at a Phenylalanine Residue in the Glycine Receptor Binding Site is Conserved for Different Agonists. *Mol Pharmacol*, 79(4):742-748.

Polenzani, L., Woodward, RM., Miledi, R. 1991. Expression of mammalian gamma-aminobutyric acid receptors with distinct pharmacology in Xenopus oocytes. *Proc Natl Acad USA, 88,* 4318-4322

Pritchett, DB., Sontheimer, H., Shivers, BD., Ymer, S., Kettenmann, H., Schofield, PR., Seeburg, PH. 1989. Importance of a novel $GABA_A$ receptor subunit for benzodiazepine pharmacology. *Nature*, 338:582-585.

Reeves, D., Lummis, SCR. 2002. The molecular basis of the structure and function of the 5-HT 3 receptor: a model ligand-gated ion channel (Review). *Mol Membrane Biol*, 19:11-26.

Roberts, E., Krause, DN., Wong, E., Mori, A. 1981. Different efficacies of d- and l-gamma-amino-beta-hydroxybutyric acids in GABA receptor and transport test systems. *J Neurosci*, 1:32-140.

Sali, A., Blundell, TL. 1993. Comparative protein modelling by satisfaction of spatial restraints. *J Mol Biol*, 234:779-815.

Schofield, CM., Jenkins, A., Harrison, NL. 2003. A highly conserved aspartic acid residue in the signature disulfide loop of the alpha 1 subunit is a determinant of gating in the glycine receptor. *J Biol Chem*, 287:34079-34083.

Sherman-Gold, R. 1993. The AXON Guide for Electrophysiology and Biophysics Laboratory Techniques, CH 3," AXON Instruments Inc. pp26-81.

Siddiqui, SZ., Brown, DDR., Rao, VTS., Forrester, SG. 2010. An UNC-49 GABA receptor subunit from the parasitic nematode *Haemonchus contortus* is associated with enhanced GABA sensitivity in nematode heteromeric channels. *J Neurochem*, 113:1113-1122.

Siddiqui, SZ., Brown, DDR., Accardi, MV., Forrrester, SG. 2012. Hco-LGC-38 is novel nematode cys-loop GABA receptor subunit. *Mol Biochem Parasit*, 185:137-144.

Sieghart, W. 1995. Structure and pharmacology of gamma-aminobutyric $acid_A$ receptor subtypes. *Pharmacol Rev*, 47:181-234.

Sigel, E., Baur, R., Kellenberger, S., Malherbe, P. 1992. Point mutations affecting antagonist affinity and agonist dependent gating of $GABA_A$ receptor channels. *EMBO J*, 11(6):2017-2023.

Simon, J., Wakimoto, H., Fujita, N., Lalande, M., Banard, EA. 2004. Analysis of the Set of GABAA Receptor Genes in the Human Genome. *J Biol Chem*, 279:41422-4435.

Sixma, TK., Smit, AB. 2003. ACETYLCHOLINE BINDING PROTEIN (AChBP): A Secreted Glial Protein That Provides a High-Resolution Model for the Extracellular Domain of Pentameric Ligand-Gated Ion Channels. *Annu Rev Biophys Biol Struct*, 32:311-334.

Smith, GB., Olsen, RW. 1994. Identification of a [^{3}H]muscimol photoaffinity substrate in the bovine gamma-aminobutyric acidA receptor alpha subunit. *J Biol*

Chem, 269:20380-20387.

Stock, JB., Rauch, B., Roseman, S. 1977. Periplasmic space in *Salmonella typhimurium* and *Escherichia coli*. *J Biol Chem*, 252(21):7850-7861.

Stroud, RM., McCarthy, MP., Shuster, M. 1990. Nicotinic Acetylcholine Receptor Superfamily of Ligand-Gated Ion Channels. *Biochem*, 29(50):11009-11023.

Tappaz, ML., Brownstein, MJ., Kopin, IJ. 1977. Glutamate decarboxylase (GAD) and gamma-aminobutyric acid (GABA) in discrete nuclei of hypothalamus and substantia nigra. *Brain Res*, 125:109-121.

Tasneem, A., Iyer, LM., Jakobsson, E., Aravind, L. 2004. Identification of the prokaryotic ligand-gated ion channels and their implications for the mechanisms and origins of animal Cys-loop ion channels. *Genome Biol*, 6:R4.

Thompson, AJ., Lester, HA., Lummis, SCR. 2010. The structural basis of function in Cys-loop receptors. *Quart Rev Biophys*, 43(4):449-499.

Thompson, AJ., Alqazzaz, M., Ulens, C., Lummis, SCR. 2012. The pharmacological profile of ELIC, a prokaryotic GABA-gated receptor. *Neuropharmacology*, 63:761-767.

Torres, GE., Egan, TM., Voigt, MM. 1999. Hetero-oligomeric assembly of P2X receptor subunits specificities exist with regard to possible partners. *J Biol Chem*, 274(19):6653-6659.

Unwin, N, Miyazawa, A., Li, J., Fujiyoshi, Y. 2002. Activation of the nicotinic acetylcholine receptor involves a switch in conformation of the alpha subunits. *J Mol Bio*, 319:1165-1176.

Unwin, N. 2005. Refined structure of the nicotinic acetylcholine receptor at 4A resolution. *J Mol Biol*, 346:967-989.

Veglia, F. 1915. The anatomy and life-history of *Haemonchus contortus*. 3rd and 4th Reports of the Director of Veterinary Research, Onderstepoort, Union of South Africa. pp347-500

Wagner, DA., Czajkowski, C., Jones, M. 2004. An Arginine Involved in GABA Binding and Unbinding But Not Gating of the $GABA_A$ Receptor. J *Neurosci*, 24(11):2733-2741.

Wegelium, K., Pasternack, M., Hiltunen, JO, Rivera, C., Kalia, K., Saarma, M., Reeben, M 1998. Distribution of GABA receptor rho subunit transcripts in the rat brain. *Eur J Neurosci*, 10:350-357.

Woodward, RM., Polenzani, L., Miledi, R. 1993. Characterization of Bicuculline/Baclofen- Insensitive (ρ-like) ɣ Aminobutyric Acid Receptors Expressed in *Xenopus* Oocytes. II. Pharmacology of ɣ-Aminobutyric $Acid_A$ and of ɣ-Aminobutyric $Acid_B$ Receptor Agonists and Antagonists. *Mol Pharmacol*, 43:609-625.

Wotring, VE., Chang, Y., Weiss, DS. 1999. Permeability and single channel conductance of human homomeric rho1 GABAC receptors. *J Physiol*, 52:327-336.

Wotring, VE., Miller, TS., Weiss, DS. 2003. Mutations at the GABA receptor selectivity filter: a possible role for effective charges. *J Physiol*, 548:527-540.

Yamamoto, I., Absalom, N., Carland, JE., Doddareddy, MR., Gavande, N., Johnston, GAR., Hanrahan, JR., Chebib, M. 2012a. Differentiating Enantioselective Actions of GABOB: A Possible Role for Threonine 244 in the Binding Site of GABAC rho1 Receptors. *ACS Chem Neurosci*, 3:665-673.

Yamamoto, I., Carland, JE., Locock, K., Gavande, N., Absalom, N., Hanrahan, JR., Allan, RD., Johnston, GAR., Chebib, M. 2012b. Structurally Diverse GABA Antagonists Interact Differently with Open and Closed Conformational States of the rho1 Receptors. *ACS Chem Neurosc*, 2:293-301.

Zhang, HG., Ffrench-Constant, RH., Jackson, MB. 1994. A unique amino acid of the Drosophila GABA receptor with influence on drug sensitivity by two mechanisms. *J Physiol*, 479(Part 1):65–75.

Zhang, D., Pan, ZH., Awobuluyi, M., Lipton, SA. 2001. Structure and function of $GABA_C$ receptors: a comparison of native versus recombinant receptors. *Trends Pharmacol Sci*, 22(3):121-132.

Zheng, W., Auerbach, A. 2011. Decrypting the sequence of structural events during the gating transition of pentameric ligand-gated ion channels based on an interpolated elastic network model. *PLOS Comput Biol*, 7:1-10.

Zhong, WG., Gallivan, JP., Zhang, YO., Li, LT., Lester, HA., Dougherty, DA. 1998. From ab initio quantum mechanics to molecular neurobiology: a cation-pi binding site in the nicotinic receptor. *Proc Natl Acad Sci USA*, 95:12088-12093.

Chapter 6: Appendices

Appendix A: Antagonists

Antagonists

APMPA

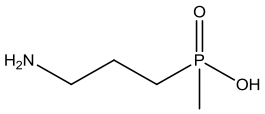

Gabazine

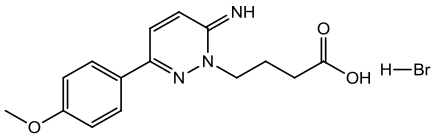

TPMPA

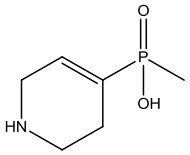

A1: Methods

3-aminopropyl (methyl)-phosphinic acid (APMPA), and 6-Imino-3-(4-methoxyphenyl)-1(6*H*)-pyridazinebutanoic acid hydrobromide (gabazine) were purchased from Tocris. (1,2,5,6-Tetrahydropyridin-4-yl)methylphosphinic acid (TPMPA) was purchased from Sigma.

The TPMPA dose-response curve was produced by fitting to the equation:

$$\frac{Iinh^{+}}{Iinh^{-}} = \frac{1}{\left(\left(\frac{[inh]}{IC50}\right)^{h}\right) + 1}$$

Where I_{inh+} is the GABA induced current in the presence of an inhibitor, I_{inh-} is the current generated solely in the presence of GABA, [inh] is the concentration of inhibitor, IC_{50} is the concentration of inhibitor required to achieve a 50% reduction of GABA response, and *h* is the Hill slope.

A1: Results

The compounds gabazine, TPMPA and APMPA exhibited no agonist activity up to 500µM, but elicited a range of inhibition of EC_{50} GABA-induced currents. At 500µM APMPA produced up to 30% inhibition on the heteromeric channel, while 100µM gabazine averaged a 57% inhibition. TPMPA, the selective $GABA_C$ antagonist, appeared to be the most potent of the three had an IC_{50} value of 54.5 ±5.1µM on Hco-UNC-49B, compared to 80.2 ±9.6µM on Hco-UNC-49BC (Figure A1).

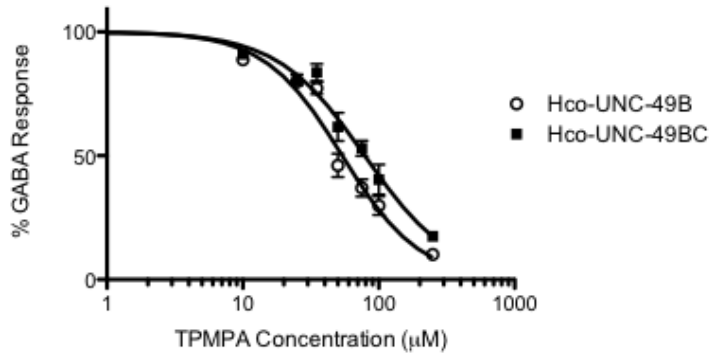

Figure A1: Inhibition curve for TPMPA at the Hco-UNC-49B and Hco-UNC-49BC receptor